Natural Environment Research Council

Institute of Geological Sciences

Mineral Reconnaissance Programme Report

A report prepared for the Department of Industry

This report relates to work carried out by the Institute of Geological Sciences on behalf of the Department of Industry. The information contained herein must not be published without reference to the Director, Institute of Geological Sciences.

D. Ostle
Programme Manager
Institute of Geological Sciences
Nicker Hill, Keyworth,
Nottingham NG12 5GG

No.61

Mineral reconnaissance at the Highland Boundary with special reference to the Loch Lomond and Aberfoyle areas

INSTITUTE OF GEOLOGICAL SCIENCES

Natural Environment Research Council

Mineral Reconnaissance Programme

Report No. 61

Mineral reconnaissance at the Highland Boundary with special reference to the Loch Lomond and Aberfoyle areas

Geology
W. G. Henderson, BA

Mineralogy
N. J. Fortey, PhD
W. G. Henderson, BA

Geophysics
C. E. Johnson, MSc

Geochemistry
A. Grout, BSc

with analytical contributions by Analytical Chemistry Unit

London 1983

A report prepared for the Department of Industry

Mineral Reconnaissance Programme Reports

15 Investigation of stratiform sulphide mineralisation at Meall Mor, South Knapdale, Argyll

16 Report on geophysical and geological surveys at Blackmount, Argyllshire

17 Lead, zinc and copper mineralisation in basal Carboniferous rocks at Westwater, south Scotland

18 A mineral reconnaissance survey of the Doon—Glenkens area, south-west Scotland

19 A reconnaissance geochemical drainage survey of the Criffel—Dalbeattie granodiorite complex and its environs

20 Geophysical field techniques for mineral exploration

21 A geochemical drainage survey of the Fleet granitic complex and its environs

22 Geochemical and geophysical investigations north-west of Llanrwst, North Wales

23 Disseminated sulphide mineralisation at Garbh Achadh, Argyllshire, Scotland

24 Geophysical investigations along parts of the Dent and Augill Faults

25 Mineral investigations near Bodmin, Cornwall. Part 1—Airborne and ground geophysical surveys

26 Stratabound barium-zinc mineralisation in Dalradian schist near Aberfeldy, Scotland; Preliminary report

27 Airborne geophysical survey of part of Anglesey, North Wales

28 A mineral reconnaissance survey of the Abington—Biggar—Moffat area, south-central Scotland

29 Mineral exploration in the Harlech Dome, North Wales

30 Porphyry style copper mineralisation at Black Stockarton Moor, south-west Scotland

31 Geophysical investigations in the Closehouse—Lunedale area

32 Investigations at Polyphant, near Launceston, Cornwall

33 Mineral investigations at Carrock Fell, Cumbria. Part 1—Geophysical survey

34 Results of a gravity survey of the south-west margin of Dartmoor, Devon

35 Geophysical investigation of chromite-bearing ultrabasic rocks in the Baltasound—Hagdale area, Unst, Shetland Islands

36 An appraisal of the VLF ground resistivity technique as an aid to mineral exploration

37 Compilation of stratabound mineralisation in the Scottish Caledonides

38 Geophysical evidence for a concealed eastern extension of the Tanygrisiau microgranite and its possible relationship, to mineralisation

39 Copper-bearing intrusive rocks at Cairngarroch Bay, south-west Scotland

40 Stratabound barium-zinc mineralisation in Dalradian schist near Aberfeldy, Scotland; Final report

41 Metalliferous mineralisation near Lutton, Ivybridge, Devon

42 Mineral exploration in the area around Culvennan Fell, Kirkcowan, south-western Scotland

43 Disseminated copper-molybdenum mineralisation near Balluchulish, Highland Region

44 Reconnaissance geochemical maps of parts of south Devon and Cornwall

45 Mineral investigations near Bodmin, Cornwall. Part 2—New uranium, tin and copper occurence in the Tremayne area of St Columb Major

46 Gold mineralisation at the southern margin of the Loch Doon granitoid complex, south-west Scotland

47 An airborne geophysical survey of the Whin Sill between Haltwhistle and Scots' Gap, south Northumberland

48 Mineral investigations near Bodmin, Cornwall. Part 3—The Mulberry and Wheal Prosper area

49 Seismic and gravity surveys over the concealed granite ridge at Bosworgy, Cornwall

50 Geochemical drainage survey of central Argyll, Scotland

51 A reconnaissance geochemical survey of Anglesey

52 Miscellaneous investigations on mineralisation in sedimentary rocks

53 Investigation of polymetallic mineralisation in Lower Devonian volcanics near Alva, central Scotland

55 Copper mineralisation near Middleton Tyas, North Yorkshire

56 Geophysical and geochemical investigations over the Long Rake, Haddon Fields, Derbyshire

57 Mineral exploration in the Ravenstonedale area, Cumbria

58 Investigation of small intrusions in southern Scotland

59 Stratabound arsenic and vein antimony mineralisation in Silurian greywackes at Glendinning, south Scotland

60 Mineral investigations at Carrock Fell, Cumbria. Part 2—Geochemical investigations

61 Mineral reconnaisance at the Highland Boundary with special reference to the Loch Lomond and Aberfoyle areas

The Institute of Geological Sciences was formed by the incorporation of the Geological Survey of Great Britain and the Geological Museum with Overseas Geological Surveys and is a constituent body of the Natural Environment Research Council

Bibliographic reference
Henderson, W. G., Fortey, N. J. and others, 1983. Mineral reconnaissance at the Highland Boundary with special reference to the Loch Lomond and Aberfoyle areas. *Mineral Reconnaissance Programme Rep. Inst. Geol. Sci.*, No. 61

Printed in England for the Institute of Geological Sciences by Imediaprint

CONTENTS

FIGURES

TABLES

SUMMARY

Serpentinite bodies at the Highland Boundary in the Loch Lomond and Aberfoyle areas are extensively altered to magnesite–quartz and ferroan-dolomite–quartz rocks. Silicification was probably initiated before conversion to carbonate. Relict textures indicate that the serpentinites were derived from peridotitic precursors, but one unaltered ultrabasic sample comprises mainly chromian diopside. Chromite geochemistry and hornblende-schist mineralogy reinforce the ophiolitic character of the serpentinite–spilite–black-shale–chert assemblage of the Highland Border.

Magnetic and VLF traverses across the Highland Boundary fracture-zone near Helensburgh identified several anomalous zones. One may be due to a concealed serpentinitic sheet.

The most mineralised serpentinite body showed chromium values in the range 1000 to 3035 ppm. Such concentrations are not encouraging for the small serpentinites at Loch Lomond and Aberfoyle, but may be significant regarding larger serpentinites elsewhere at the Highland Border.

INTRODUCTION

The Highland Boundary Fracture Zone and adjacent rock units can be regarded as a potentially mineralised geological feature for the following reasons:

1 The ultrabasic rocks, particularly the serpentinites, may contain concentrations in Cr, Ni and platinum group metals.

2 Base metal elements, especially Cu, may be concentrated in ophiolitic rocks.

3 The Fracture Zone, acting as a major lineament in the earth's crust, may have channelled metal-bearing solutions or provided a suitable depositional environment for metalliferous fluids.

SCOPE OF PROJECT

A desk evaluation of published literature, undertaken in December 1977, indicated that the Highland Border rocks might best be studied in the Loch Lomond and Aberfoyle areas (Figure 1). Geological accounts and maps (e.g. Jehu and Campbell, 1917) showed that these areas contain all of the rock types found elsewhere in association with the Highland Boundary Fracture Zone. Initial field and petrographic studies attempted to elucidate the history of the Highland Border rocks. Over 100 thin sections supplied petrographic data which helped to interpret the complex lithologies. Rock geochemistry established metal values in the only exposures found to be significantly mineralised. Geophysical surveys west of Loch Lomond investigated major faults and altered serpentinite bodies.

The areas discussed in this report lie within a larger area at the Highland Border where drainage geochemical sampling has recently been carried out. These geochemical results will be presented separately at a later date.

GENERAL GEOLOGY OF THE LOCH LOMOND AND ABERFOYLE AREAS

The term 'Highland Border rocks' covers the varied rock assemblage exposed as a NE–SW belt between the Lower Old Red Sandstone and the Southern Highland Group (Dalradian). The term includes all sedimentary, igneous and metamorphic rocks and their altered equivalents, but not igneous or sedimentary rocks of Devonian or later age.

The Highland Border rocks form a discrete mappable unit along the south-east margin of the Grampian Highlands (Figure 1). This distinctive rock unit was recognised from the turn of the century by the Geological Survey on one-inch Sheet 38 (Loch Lomond) and by Barrow (1901) in Forfarshire and Kincardineshire. Campbell (1913) described the Stonehaven section and Jehu and Campbell (1917) the exposures near Aberfoyle. At Balmaha, Loch Lomond, altered serpentinite occurs in two north-east trending belts designated 'northern' and 'southern' (Figure 2).

The Dalradian rocks at the Highland Border are cleaved greywackes, siltstones and slates of greenschist metamorphic facies. Shackleton (1957) appreciated that the main cleavage is downward-facing and related to an inverted major fold, the Aberfoyle anticline. In the Loch Lomond and Aberfoyle areas the hinge of this fold passes through the Aberfoyle and Luss Slates, which are laterally equivalent to the Dunoon Phyllites. These slates are grey-green, blue and purple in colour. Cleaved greywackes and cleaved fine conglomerates, which Shackleton (1957) correlated with the Leny Grits, occupy an extensive tract of

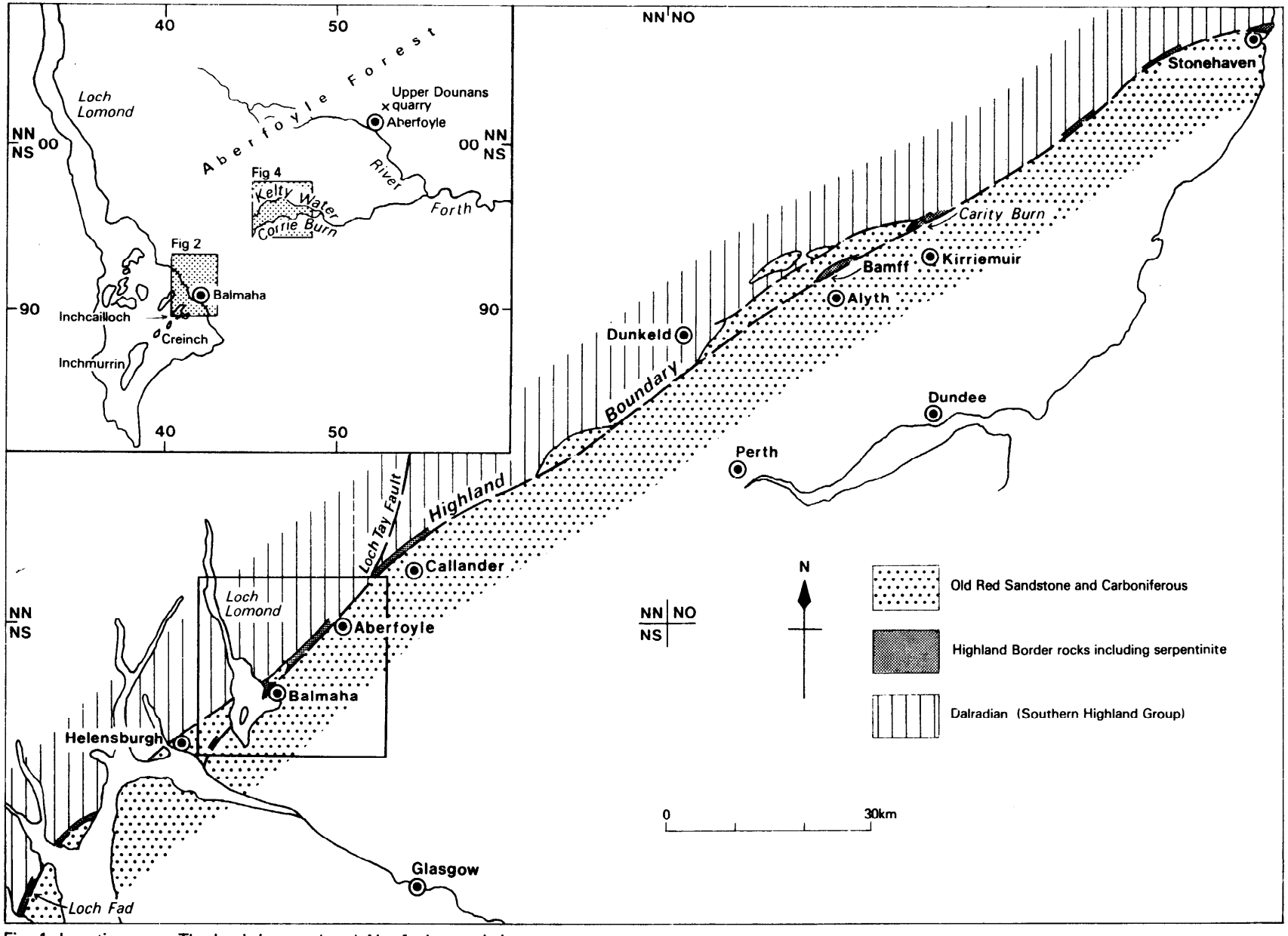

Fig. 1: Location map. The Loch Lomond and Aberfoyle area is inset

ground south-east of the slates. The Leny Grits contain a number of relatively thin bands of purplish slate. Bedding is not always recognisable, but from place to place clear sedimentary structures such as grading, ripple-drift cross-lamination, loading and channellised features show the direction of younging. Harris and Pitcher (1975) include the Dalradian rocks of the Highland Border in the Southern Highland Group, which is thought to be of Lower Cambrian age.

Close to the Highland Boundary the Lower Old Red Sandstone comprises lithic sandstones, conglomerates and minor siltstones and has a steep south-east dip. In the Loch Lomond and Aberfoyle areas the upturned edges of conglomerate and sandstone units form prominent topographic features, such as the higher parts of the islands of Inchmurrin, Creinch and Inchcailloch in Loch Lomond, Conic Hill, and the Monteith Hills east of Aberfoyle.

The great thickness of the Lower Old Red Sandstone in the Midland Valley and the steep dip along the Highland edge signify a considerable south-east downward displacement along the Highland Boundary Fault Zone. The same fault-zone, however, displaces Upper Old Red Sandstone rocks down to the north-west against Lower Old Red Sandstone at Loch Lomond. Therefore, the main post-Lower Old Red Sandstone faulting was of mid-Devonian age. Lateral fault-movements may have accompanied these dip-slip displacements since numerous north-east trending wrench faults, such as the Loch Tay Fault, run at low angles into the Highland Boundary (Anderson, 1942; Anderson, 1947).

The Highland Border rocks comprise a varied assemblage, including serpentinite (and altered equivalents), spilitic igneous rock, black phyllite, chert and sandstone. Many lithological contacts are tectonic. Most of the rocks are foliated or cleaved. Henderson and Fortey (1982) show that earlier deformational and metamorphic effects remain visible despite mid-Devonian and later faulting at the Highland Boundary. In the Loch Lomond and Aberfoyle areas, rocks representing different sedimentological, deformational and metamorphic processes occur together. As an example, garnetiferous hornblende-schists in the Aberfoyle Forest are considerably more deformed and metamorphosed than adjacent black slates or nearby regionally-metamorphosed Leny grits.

ROCKS OF ULTRABASIC ORIGIN

The ultrabasic rocks, well displayed in the two serpentinite belts at Balmaha (Figure 2), are generally strongly altered. Repeated veining and brecciation accompanied the conversion of serpentinites to carbonate-quartz rocks and jasper. For convenience of description, alteration to carbonate mineralogies is termed carbonatisation.

ORIGINAL NATURE OF ULTRABASIC ROCKS

In both the northern and southern belts at Balmaha there are a number of localities where the earlier mineralogy has not been greatly modified to carbonate and silica minerals. In the following four descriptions all but the last refer to the northern of the two belts.

1 Tectonised serpentinite occurs at the south-west end of a small crag 170 m north-east of Arrochymore Point [NS 4102 9190]. Steeply dipping ramifying fractures bound angular wedge-shaped areas of massive serpentinite. Of three main serpentine textures the most dominant is mesh-texture, which probably mimics olivine grains. Bastite serpentine texture, probably after pyroxene, is less abundant. The third texture, fibrous serpentine, infills veinlets. XRD showed the serpentine minerals to be antigorite, lizardite and chrysotile. Large grains of deep brown translucent spinel (chromite) are ubiquitous.

2 In the small islet 120 m NNE of Arrochymore Point [NS 4094 9189], highly tectonised serpentinite contains subrounded cobble-sized fragments. A foliated matrix consists of serpentine, locally with carbonate and talc. Mesh and bastite textures and chromite grains are similar to those at locality (1). XRD indicates that chrysotile (clinochrysotile) which has both a platy and a fibrous habit, makes up most of one of the fragments.

3 In 1978, Mr I. H. Hall (Institute of Geological Sciences) sampled a compact green block from within schistose serpentinite at the back of a low cliff-feature 190 m north-east of Arrochymore Point [NS 4101 9193]. Slipped superficial material now covers the exposure. The sample proved to be a coarsely granular pyroxenite containing pockets of 'serpentine' and a strongly pleochroic talc–chlorite. The texture is slightly mylonitic and the pyroxenes display strongly curved exsolution lamellae. Table 1 gives six microprobe analyses of pyroxenes and accompanying chlorite minerals. The pyroxene, a low-titanium diopside with a moderate chromium content, compares with pyroxene from ultramafic igneous rocks (Deer and others, 1978). Diopside of metamorphic origin is rarely chromian.

4 Serpentinite, only slightly altered to carbonate, occurs in the southern belt 770 m south-west of the summit of Conic Hill [NS 4254 9212]. The weakly foliated serpentinite here consists of rounded pebble-like fragments set in a matrix of finer subrounded grains with average diameter of 2 mm. XRD showed that lizardite is the sole serpentine mineral of two separate grains. Bedding traces appear at two localities and Henderson and Fortey (1982) consider that much of the southern serpentinite belt originated as a rudaceous sediment.

Judging from the proportion of relict mesh

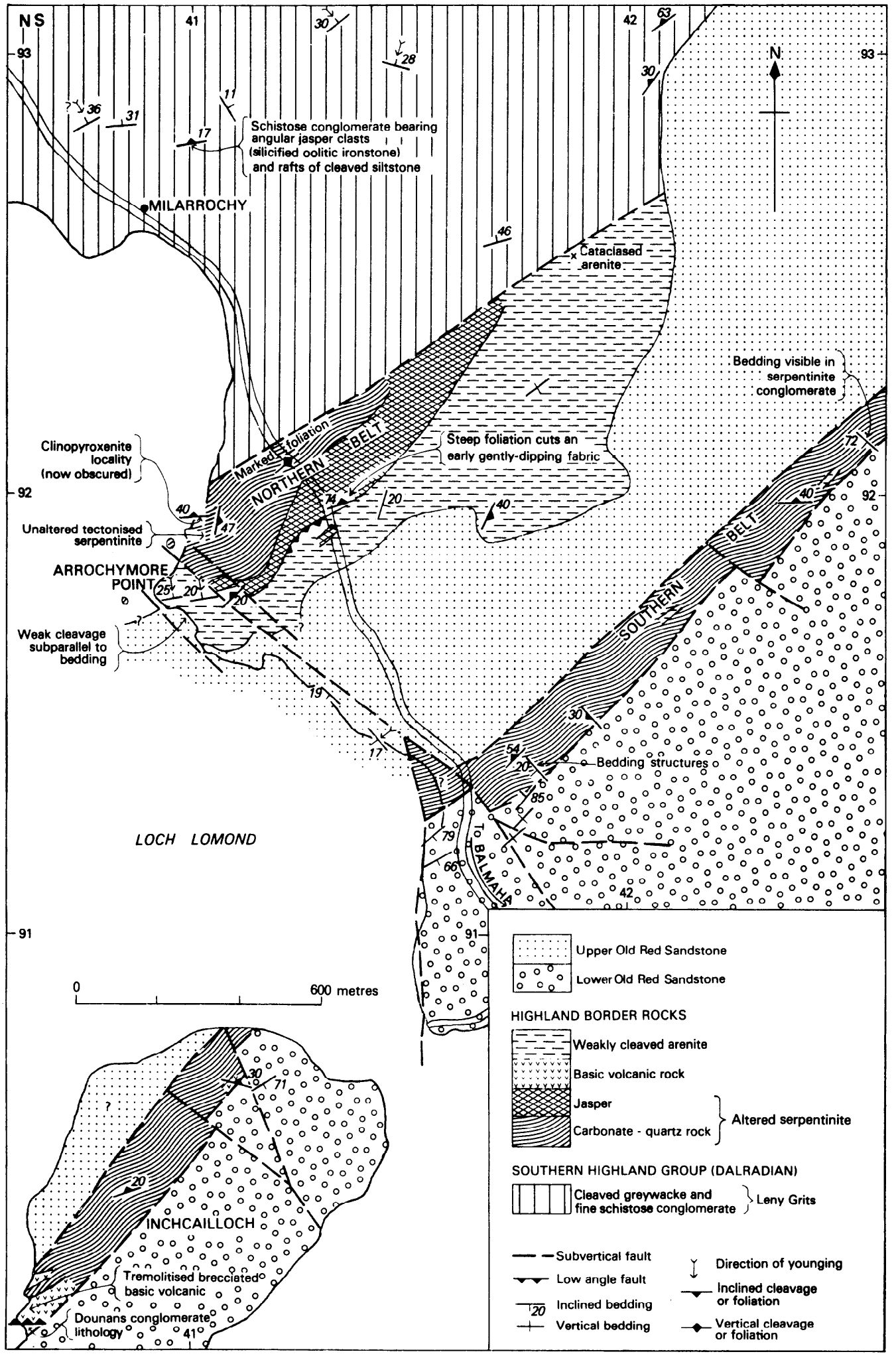

Fig. 2: Geology of the Highland Boundary at Balmaha, Loch Lomond.

TABLE 1

Electron microprobe analyses of diopside and accompanying chlorite in pyroxenite from Balmaha, Central Scotland (Analyst B. Beddoe-Stephens).

PTS 4790	Diopside						Chlorite	
Analyses	1	2	3	4	5	6	7	8
SiO_2	52.07	52.21	52.75	51.95	52.96	52.61	36.66	34.54
TiO_2	0.16	0.11	0.12	0.10	0.06	0.10	0.00	0.00
Al_2O_3	3.32	3.17	2.87	3.60	2.57	3.04	4.51	9.73
Cr_2O_3	0.41	0.36	0.36	0.45	0.34	0.43	0.30	0.86
FeO*	4.18	3.82	3.61	3.98	3.77	3.73	7.23	6.64
MnO	0.10	0.03	0.01	0.05	0.07	0.04	0.07	0.00
MgO	15.69	15.94	15.99	16.12	17.06	16.73	35.47	35.36
CaO	24.55	25.28	25.36	24.98	25.05	25.15	0.06	0.04
Na_2O	0.03	0.03	0.01	0.05	0.03	0.02	0.00	0.00
K_2O	not analysed for							
Total	100.51	100.95	101.08	101.28	101.91	101.85	84.30	87.17
Si	1.905	1.902	1.916	1.887	1.909	1.898	7.296	6.642
Ti	0.004	0.003	0.003	0.003	0.002	0.003	0.000	0.000
Al	0.143	0.136	0.123	0.154	0.109	0.129	1.058	2.205
Cr	0.012	0.010	0.010	0.013	0.010	0.012	0.047	0.131
	2.064	2.051	2.052	2.057	2.030	2.042		
Fe	0.128	0.116	0.110	0.121	0.114	0.113	1.203	1.068
Mn	0.003	0.001	0.000	0.002	0.002	0.001	0.012	0.000
Mg	0.855	0.865	0.865	0.873	0.917	0.900	10.522	10.135
Ca	0.962	0.987	0.987	0.972	0.967	0.972	0.013	0.008
Na	0.002	0.002	0.001	0.004	0.002	0.001	0.000	0.000
	1.950	1.971	1.963	1.972	2.002	1.987		
No of 'O's per unit cell	6	6	6	6	6	6	28	28
Ca	49.5	50.2	50.3	49.4	48.4	49.0		
Fe	6.6	5.9	5.6	6.2	5.7	5.7		
Mg	43.9	43.9	44.1	44.0	45.9	45.3		

*Total Fe expressed as FeO

Analyses were carried out on a Cambridge Instruments Microscan 5 microprobe. Measurements were made with a beam potential of 15 kV using pure metal standards for Ti, Cr, Fe and Mn, and wollastonite, olivine, jadeite and orthoclase standards for other elements

TABLE 2

Identification of carbonates in carbonate-quartz rocks

Sample Number	Locality	METHOD XRD	Stain	Infra-red
BX645	Northern Belt	Dolomite/ankerite	-	-
		" "	-	-
S.65451	" "	-	Ferroan dolomite/ankerite	-
BX771	" "	Dolomite/ankerite	-	-
BX776	" "	Baryte confirmed	Ferroan dolomite/ankerite	-
S.65457	" "	Dolomite/ankerite	" " "	-
S.65463		" "	-	-
BX831	" "	-	" " "	-
BX832	" "	Dolomite/ankerite	-	Dolomite (not ankerite)
BXNJ1	" "	-	-	" " "
BXNJ2	" "	-	Ferroan dolomite/ankerite	-
BXNJ5	" "	-	" " "	-
BXNJ5A	" "	Dolomite/ankerite	" " "	-
BX651	Southern Belt	Magnesite	Magnesite	Magnesite with traces of dolomite (and quartz) cut by veinlets of magnesite
BX653	" "	-	-	Magnesite (and quartz) with trace of dolomite cut by dolomite veinlets themselves cut by magnesite veins.
BX774	" "	Magnesite	-	Magnesite cut by veins of magnesite
S.65678	" "	Magnesite	Magnesite veined by ferroan dolomite/ankerite	-
S.67397	" "	-	Ferroan dolomite/ankerite	-
S.67489	Lime Hill, 7 km SW Aberfoyle	Magnesite	-	-
S.67488	Upper Dounans, Aberfoyle	Dolomite/ankerite	-	-
S.65465	Inchcailloch	Dolomite/ankerite	Ferroan dolomite/ankerite	-
S.65466	"	-	" " "	-

(a) XRD by powder photography (D Atkin, B R H Skilton and W G Henderson) distinguishes magnesite from dolomitic carbonates but is poor at distinguishing varieties in the dolomite-ankerite series.

(b) Staining by B R H Skilton using methods described by Hutchison (1974). Alizarin Red distinguishes dolomite or magnesite from calcite and ankerite/ferroan dolomite. Specimens which showed no colour reaction at this stage were stained with Magneson Solution to distinguish dolomite from magnesite.

(c) Infra-red analysis by D J Bland with a Perkin-Elmers 577 spectrophotometer. This technique distinguishes all the carbonates encountered here.

TABLE 3

Microprobe Analysis of Alteration to Chromite Grain

SiO_2	0.93
TiO_2	0.04
Al_2O_3	0.07
Cr_2O_3	2.67
FeO*	84.58
MnO	0.09
MgO	< 0.01
CaO	< 0.01
NiO	0.73
Total	89.12

* Total Fe expressed as FeO. Regarding the iron as Fe_2O_3 improves the total, but still leaves about 5% unaccounted for. H_2O could be present in appreciable amounts, however.

Analysis by N J Fortey at IGS, Grays Inn Road, London.

Sample (BX653; PTS4787) from old quarry on Tom nan Oisgean, 605 m NE of the Old Manse, Balmaha [NS 4209 9171].

TABLE 4

Partial chemical analyses of altered serpentinites, Loch Lomond

	Southern Belt	Northern Belt				Inchcailloch	
	Carbonate-Quartz Rock	Carbonate-Quartz Rocks		Jaspers		Carbonate-Quartz Rocks	
	S.35523-6	BX 776	S.65457	S.65458	PTS 4788	S.65465	S.65466
	Lab. No. 1343						
SiO_2	39.1	2.27	2.24	very high (> 98%)	98.4	47.0	61.5
Al_2O_3	1.8(approx)	0.01	0.05	0.09	0.23	0.22	0.55
Total iron as Fe_2O_3	5.4	6.21	9.26	2.05	2.01	3.34	4.86
MgO	12.4	15.7	14.7	0.15	0.09	13.1	12.3
CaO	15.0	16.3	19.0	0.02	0.0	10.1	15.1
K_2O		0.03	0.05	0.04	0.14	0.08	0.06
TiO_2	Trace	0.01	0.01	0.0	0.0	0.01	0.01
$H_2O < 105^oC$	0.4						
CO_2	24.7						
Mn	1000(approx)	2469	2435	0	0	467	986
P_2O_5	Trace						
Zr		0	0	0	0	0	0
B		0	0	20	27	0	3
Cr*		1120	2140	1060	1000	1510	1670
Cr	3000(approx)	999	1703	1554	945	886	987
V		71	111	0	55	37	13
Ni†		340	440	10	10	480	70
Ni		623	941	73	364	514	462
Co†		55	55	5	5	45	40
Co		95	121	18	5	45	44
Ba	Trace	5782	131	1663	> 9999	68	416
Li		6.1	6.9	17.2	17.4	18.7	21.8
Rb		2	3	0	0	3	0
Be		0.8	0.0	0.3	3.4	0.1	0
Cu†		60	50	10	15	10	20
Cu		33	29	41	28	2	18
Sr	Trace(approx)	1045	1016	35	894	477	177
Y		3	2	0	2	0	0
La		57	54	0	0	55	7
Pb†		20	20	0	10	10	10
Zn†		40	50	0	10	20	20

C O Harvey analysed sample S.35523-6 in September 1943 presumably by wet chemical methods, excepting those qualified by "approx" which are partly based on spectrographic work by J A C McClelland. Analyses of the other samples were made predominantly by direct-reading optical emission spectrometry by A R Date in June 1979. Other values were determined by B S Chaumoo in July 1979; those marked with an asterisk (*) utilised inductively coupled plasma direct-reading spectrometry and those marked with a dagger (†) utilised atomic absorption spectrometry.

textures to relict bastite textures the original ultrabasic rocks were mainly peridotitic in composition with pyroxenitic variants.

CARBONATISATION AND SILICIFICATION

Ultrabasic bodies at the Highland Border are largely altered to carbonate–quartz rock. Such rock commonly shows a complex internally-foliated or fragmental texture which varies from locality to locality. Textural differences are brought out by changes in mineralogy (from carbonate to quartz, for example); grain-size; grain shape, for example from polygonal mosaic textures to textures with raggy indeterminate grain boundaries; distribution of fine opaques such as hematite and magnetite; and veining sequence.

Silica minerals vary from very abundant in the jaspers to virtually absent in carbonate dominated rocks. Both carbonate and quartz pseudomorph bastite and mesh textures; the distribution of fine opaque grains enhances relict textures. There are two main carbonate minerals, magnesite and ferroan dolomite/ankerite. Calcite appears to be restricted to certain late fracture fills. The carbonate of the northern belt at Balmaha is generally dolomitic but magnesite predominates in the southern belt (Table 2).

The carbonate minerals form granules, radiating sheaves and comb structures. The silica minerals also exhibit textural variability. In many samples, quartz with extreme undulose extinction has a ragged crystal form and indistinct grain boundaries. In some others a fine quartz mosaic comprises polygonal grains with normal extinction behaviour. Chalcedonic quartz fibres form radiating sheaves filling vein-like structures and probably mimic curvilinear serpentine minerals. Coarse granular quartz also fills late veins.

Deep brownish-red chromite grains abound in both carbonate–quartz rocks and jaspers. They show distinctive alteration, peripherally and along fracture surfaces, to an opaque phase which is optically anisotropic and homogenous. One microprobe analysis of this material, given in Table 3, has a low total weight % which might be due to an appreciable H_2O content. Many chromite grains are also rimmed by a halo of fine grained green (? chromian) mica or chlorite. Green phyllosilicate minerals also lie on many fracture surfaces in carbonate–quartz rock and jasper. Examination of this green material by X-ray powder photography (D. Atkin) revealed a di-octohedral kaolinite-group mineral with quartz and minor magnesite, plus a minor phase, probably an interlayered clay mineral. A second specimen examined by X-ray diffractometry following glycerol treatment (E. Georgiou and D. J. Morgan) showed 'Mica with a broad (001) peak at 10.4 Å unaffected by glycerol'. A preliminary qualitative XRF-scan of this material detected anomalous Cr and Ni (Cr>Ni). Therefore it is probably an inhomogenous mixture of chromian mica (fuchsite) and clays bearing some nickel.

Talc–dolomite–serpentine assemblages demonstrate that the introduction of CO_2 progressively altered the serpentinites to carbonate–quartz rocks. An extensive literature describing such alteration includes Wellman (1942), Bailey and Everhart (1964), Groves and others (1974) and Eckstrand (1975).

In the jaspers, a fine quartz mosaic perserves detailed serpentine-like textures, but no relict carbonate textures are seen. Although some jaspers could have had carbonated precursors, most were probably derived directly by silicification of serpentinite. Carbonate–quartz rock in the southern belt includes fine-grained quartzose patches. These patches pre-date the carbonate component and also formed directly from serpentinite.

CHEMISTRY

Narrow streaks and small lenses of non-sulphide ore minerals lie in strongly foliated carbonated serpentinite in the northern belt at Balmaha. The first sample collected (BX 645) contained chromite grains surrounded and veined by hematite. Qualitative XRF scanning detected major Sr, Fe, Mn and Cr with minor Ni, Cu and Ba.

Following this identification of chromite, carbonate–quartz rock of the northern belt was sampled at 1 m intervals across its exposure in the cut for the Balmaha–Rowardennan road. Two of these samples, together with two samples of jasper from the northern belt and two carbonate–quartz rocks from Inchcailloch, were analysed by optical emission spectrometry (Table 4; Figure 5). Cr values were checked by plasma emission spectrometry (Table 4) and this method was also applied to four other samples from the road cut (Table 5). Plasma emission spectrometry, a highly stable technique, may achieve results with a precision approaching 1% (see Tables 4–5).

Table 5 Cr values of carbonated serpentinite in Northern Belt at Balmaha, Loch Lomond (in ppm).

BX 789	BX 790	BX 802	BX 804
1709	2840	3035	1660

Samples analysed by inductively coupled plasma optical emission spectrometry (L. Ault).

Cr values in these samples fall in the range 1000 to 3035 ppm. These results were used as standards to calibrate values obtained by a portable X-ray fluorescence analyser on the remaining 27 samples from the road cut. The calibration curve in Figure 3 was estimated by eye. Since this analytical method is useful in the field it is described in full:

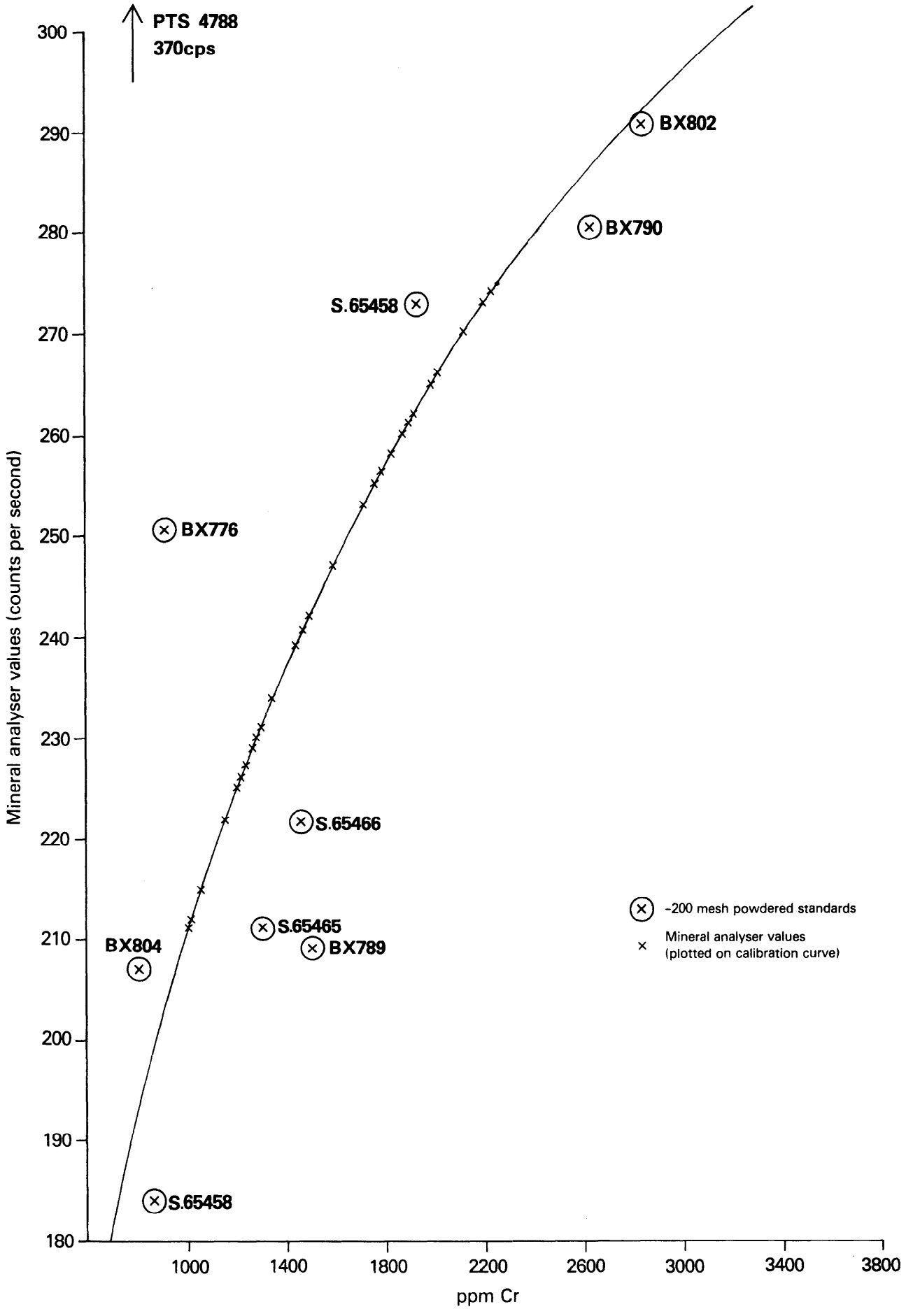

Fig. 3 Calibration curve for converting values obtained by portable XRF mineral analyser on altered Highland Border Serpentinites to Cr concentrations.

An Fe^{55} radioisotope source is probably best for excitation of CrKα radiation but, as it was not available, a Pu^{238} source was used. Pu^{238} has principal photon energies approximately twice those of Fe^{55} which can cause excessive excitation of Mn and Fe, depending on the type of matrix. A Pu^{238} source, however, has been successfully used in Cr analysis elsewhere (Johnson and others, 1980). The errors in the XRF analyses (Figure 3) are probably due to matrix effects. The precision, calculated from the mean of three readings per sample at 95% confidence limits, varies from ± 200 ppm for a Cr content of 1060 ppm to ± 800 ppm for a Cr content of 3035 ppm. Samples having more than 5% total Fe show spuriously high chromium values. For example, sample PTS 4788 (20.1% total Fe) gave a count reading corresponding to over 4000 ppm Cr, whereas the rock only contains 900–1000 ppm (Table 4). The data are generally insufficient for correction factors for Fe and Mn content to be rigorously applied.

The range of chromium values indicated by the portable XRF analyser is between 1250 and 2450 ppm and falls within the range determined by emission spectrometry. Chromium values in these altered serpentinites, therefore, are not especially high. Groves and others (1974) showed that Cr is lost from serpentinites during conversion to carbonate–quartz rocks. The chromian phyllosilicate growths in fractures and around chromite grains demonstrate that the Highland Border serpentinites have also suffered movement, and probable loss of Cr during alteration.

Chromite composition can be used as a petrogenetic indicator (Irvine, 1967), and Table 6 shows microprobe analyses of chromites from the Highland Border. The large variation in the Al and Cr content of the analysed chromites is similar to that in ophiolitic assemblages (e.g. Irvine, 1967; MacGregor and Basu, 1979). Note that within the same sample of altered serpentinitic sediment (PTS 3787) there are two grains of markedly differing compositions.

HORNBLENDE-SCHISTS

A strip of hornblende-schists, approximately 3.5 km long and 100 m to 150 m wide, outcrops in the Aberfoyle Forest (Figure 4). The hornblende-schists are accompanied by chlorite-schists and probably were derived in part from spilitic lavas (Jehu and Campbell, 1917) and in part from laminated volcaniclastic rocks. The hornblende-schists have an S–tectonite fabric formed by the growth of acicular green amphibole. The amphibole, generally fresh, is accompanied by plagioclase and epidote with accessory sphene. One small locality in the Corrie Burn shows abundant garnets (Jehu and Campbell, 1917). Table 7 shows microprobe analyses of twelve amphiboles and two sphenes (samples located on Figure 6). According to the classification of Papike and others (1974), the amphibole is pargasite.

These hornblende-schists are more highly metamorphosed and deformed than nearby Dalradian metasediments, which are of greenschist facies. Henderson and Fortey (1982) favour a dynamothermal origin, likening the hornblende-schists to those often associated with allochthonous ophiolite sheets (e.g. Spray and Williams, 1980; Jamieson, 1980).

GREENSTONES

Although Jehu and Campbell (1917) described spilites from the Aberfoyle area, the available exposures are now limited and the authors have not systematically re-examined them. On the island of Inchcailloch, however, Anderson (1947) drew attention to a well-exposed spilitic volcanic rock. The rock is tough, green and fine grained with a range of pebble-like, pillow-like and brecciated internal structures. It is extensively altered to felted areas of tremolitic amphibole intergrown with chlorite and contains veins and patches of clear unstrained albite and carbonate.

Similar mineralogies are also found on Creinch, another island in Loch Lomond (Figure 1) as alteration products of a volcaniclastic rudite. Table 8 gives four microprobe analyses of the Creinch amphiboles. Although the totals are low the amphiboles are clearly tremolitic.

GEOPHYSICAL SURVEYS IN THE HELENSBURGH AREA

Four lines, each about 1.5 km long, were surveyed in 1978 in the Highland Boundary Fracture Zone near Helensburgh (Figure 7) using a Geometrics proton magnetometer and a Geonics EM16 VLF instrument. In the Helensburgh area the Fracture Zone comprises two major fault-lines. Lines 1 and 4 transected the southern fault-line, which separates Lower Old Red Sandstone to the south from Upper Old Red Sandstone to the north (Figure 8). On line 1 a band of altered serpentinite about 140 m wide lies within this fault-line. Lines 2 and 3 cut across the northern fault-line, which divides Upper Old Red Sandstone to the south from Dalradian metasediments.

The aims of the geophysical surveys were to establish lithological control by means of line 1, and to indicate possible occurrences of concealed serpentinite in other sections of the Fracture Zone.

TABLE 6

EPMA Analyses for Chromites from the Balmaha area

(Analyst N J Fortey)

Specimen / Polished thin-section		PTS4795(BX812)				PTS4789(BX831)				PTS4787(BX653)				PTS5005(BXNJ4)				
	Analysis	1	2	3	4	5	6	7	8	9	10	11	12	13	14	15	16	17
Weight Percentages	SiO_2	0.10	0.07	0.08	0.08	0.08	0.09	0.09	0.10	0.09	0.07	0.11	0.12	0.06	0.06	0.11	0.04	0.06
	TiO_2	0.02	0.03	0.01	0.02	0.07	0.06	0.05	0.07	0.01	0.01	0.02	0.04	0.05	0.03	0.06	0.05	0.04
	Al_2O_3	20.23	20.54	22.00	21.62	8.27	9.09	9.44	9.79	32.08	32.11	15.51	15.55	32.96	29.95	29.68	29.12	30.54
	Cr_2O_3	49.27	49.33	49.42	49.68	60.49	58.98	58.68	58.02	37.92	38.21	53.77	54.48	37.82	40.32	40.12	40.53	39.16
	FeO*	18.05	17.83	16.52	16.71	19.23	19.67	20.31	20.58	14.56	14.32	20.52	20.22	15.78	15.01	16.60	16.66	16.09
	MnO	0.31	0.31	0.33	0.31	0.34	0.35	0.33	0.37	0.26	0.25	0.42	0.37	0.26	0.30	0.36	0.36	0.46
	MgO	10.75	10.76	9.03	11.79	10.35	10.48	10.10	10.04	14.61	14.67	9.15	9.24	13.10	13.04	12.53	12.38	12.22
	NiO	0.07	0.08	0.06	0.07	0.09	0.10	0.12	0.07	0.07	0.15	0.09	0.08	0.09	0.10	0.10	0.11	0.08
	Total	98.80	98.95	97.45	100.28	98.92	98.82	99.12	99.04	99.65	99.79	99.59	100.10	100.12	98.81	99.46	99.23	98.65

*Total iron expressed as FeO

Formulae based on $2R^{III}.R^{II}.O_4$	Si	.003	.002	.003	.002	.003	.003	.003	.003	.003	.002	.004	.004	.002	.002	.003	.001	.002
	Ti	.000	.001	.000	.000	.002	.002	.001	.002	.000	.000	.000	.001	.001	.001	.001	.001	.001
	Al	.756	.767	.828	.789	.326	.357	.370	.384	1.110	1.109	.595	.593	1.140	1.049	1.050	1.036	1.085
	Cr	1.235	1.235	1.247	1.216	1.601	1.554	1.542	1.526	.880	.885	1.383	1.394	.877	.947	.952	.968	.933
	Fe^{III}	.021	.000	.000	.000	.069	.084	.082	.085	.008	.003	.018	.008	.000	.001	.000	.000	.000
	Fe^{II}	.458	.472	.441	.433	.469	.464	.488	.487	.350	.348	.540	.539	.387	.411	.417	.421	.405
	Mn	.008	.008	.009	.008	.010	.010	.009	.010	.006	.006	.012	.010	.006	.008	.009	.009	.012
	Mg	.508	.508	.430	.544	.516	.521	.500	.498	.639	.641	.444	.446	.573	.578	.560	.557	.549
	Ni	.002	.002	.002	.002	.002	.003	.003	.002	.003	.004	.002	.002	.002	.002	.002	.003	.002
	Total 4-valent cations	.003	.003	.003	.002	.005	.005	.004	.005	.003	.002	.004	.005	.003	.003	.004	.002	.003
	Total 3-valent cations	2.012	2.002	2.075	2.005	1.996	1.995	1.994	1.995	1.998	1.996	1.996	1.995	2.017	1.997	2.002	2.004	2.018
	Total 2-valent cations	.976	.990	.882	.987	.997	.998	1.000	.997	.998	.999	.998	.997	.968	.999	.988	.990	.968
	Total cations	2.991	2.995	2.960	2.994	2.998	2.998	2.998	2.997	2.999	2.997	2.998	2.997	2.988	2.999	2.994	2.996	2.989
Ratios based on formulae	$100xCr/(Cr+Al)$	62.03	61.69	60.10	60.65	83.08	81.32	80.65	79.90	44.22	44.38	69.92	70.16	43.48	47.44	47.55	48.30	46.23
	$100xMg/(Mg+Mn+Ni+Fe^{II})$	52.05	51.31	48.75	55.12	51.76	52.20	50.00	49.95	64.03	64.16	44.49	44.73	59.19	57.86	56.68	56.26	56.71
	$100xFe^{III}/(Al+Cr+Fe^{III})$	1.04	0.0	0.0	0.0	3.46	4.21	4.11	4.26	0.40	0.15	0.90	0.40	0.0	0.05	0.0	0.0	0.0

Notes (a) in this table, two analyses were made on the same grain. Thus in PTS 4795 two grains were analysed.

(b) in calculating formulae iron was apportioned by the following equations:

$$X_{Fe}{}^{III} = {}^{2}/_{3}(X_{Fe_M} + X_{Mn} + X_{Mg} + X_{Ni}) - {}^{1}/_{3}(X_{Al} + X_{Cr})$$

$$X_{Fe}{}^{II} = X_{Fe_M} - X_{Fe}{}^{III}$$

where X_{Mn} etc. refer to atomic proportions i.e. wt% element/atomic wt. element.

X_{Fe_M} is wt% total iron/atomic wt. iron.

(In some cases $X_{Fe}{}^{III}$ proved to be negative and here all Fe is given as Fe^{II})

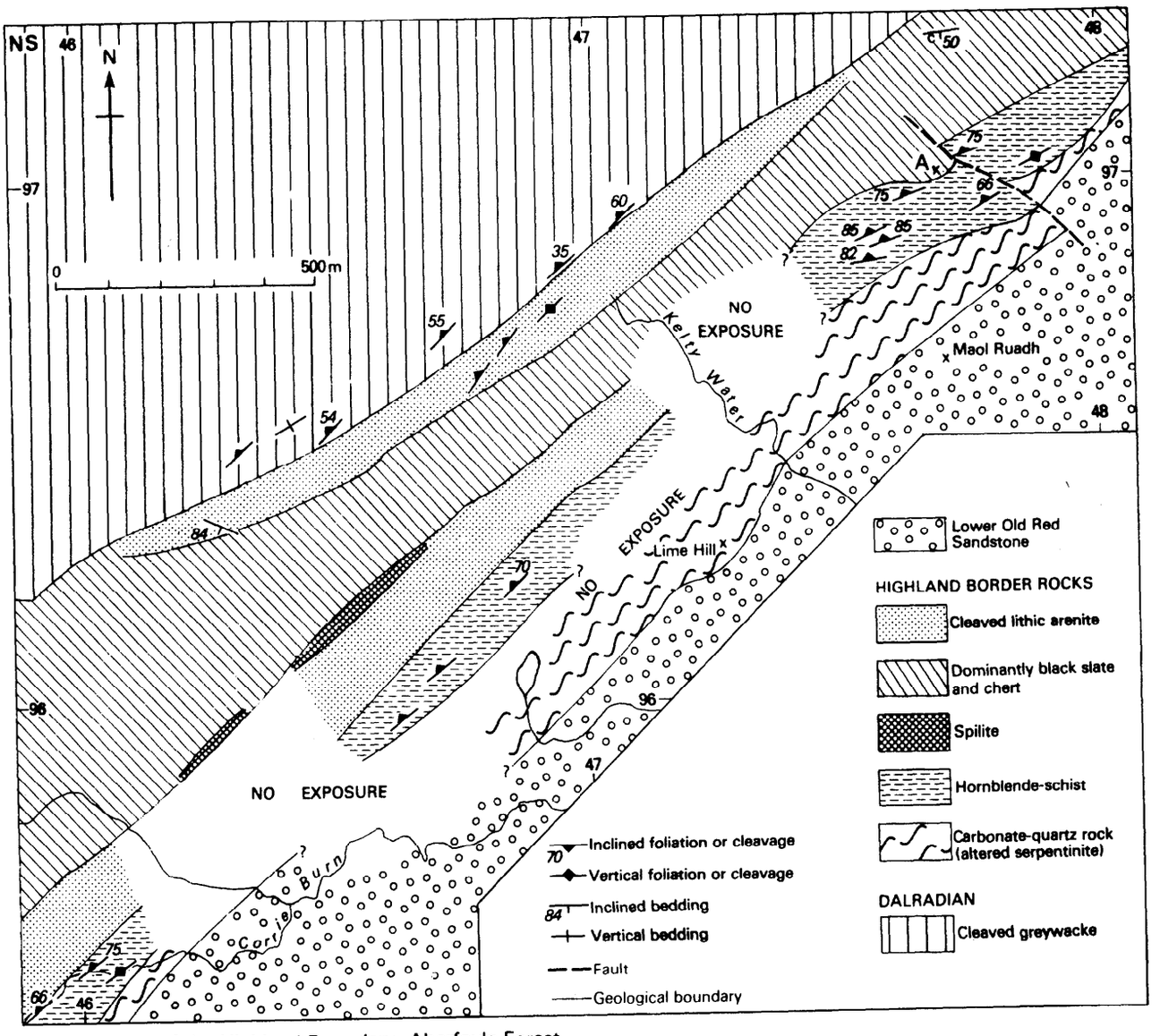

Fig 4: Geology of the Highland Boundary, Aberfoyle Forest.

TABLE 7

Composition of Hornblendes (analyses 5-13, 15-17) and Sphenes (analyses 14, 18) from Hornblende-schists in the Aberfoyle Forest

(Analyst M J Fortey)

* Total Fe expressed as FeO

Specimen no.	PTS5349 (EX1150)			PTS5437 (EX1059)			PTS5435 (EX1037)			PTS5438 (EX1071)			PTS5438 (EX1071)	
Analysis	5	6	7	8	9	10	11	12	13	15	16	17	14	18
SiO_2	45.97	44.29	47.72	44.30	45.86	43.91	46.66	43.98	43.23	41.94	43.05	43.24	29.48	24.86
TiO_2	0.34	0.48	0.29	0.61	0.55	0.65	0.34	0.48	0.63	0.81	0.78	0.79	40.13	40.37
Al_2O_3	10.25	11.56	9.18	11.40	11.38	11.56	10.24	10.73	11.82	12.29	11.12	10.87	1.24	1.36
Cr_2O_3	0.05	0.09	0.10	0.05	0.01	< .01	0.02	0.01	0.02	0.02	0.04	0.06	0.03	0.05
FeO*	12.72	13.81	11.99	15.98	15.93	15.48	14.39	14.90	15.03	14.97	15.01	14.86	0.41	0.44
Fe_2O_3 calc	2.34	2.72	1.11	2.49	3.11	2.68	0.55	3.34	5.15	2.29	2.23	1.37		
FeO calc	10.61	11.37	10.99	13.74	13.13	13.07	13.90	11.90	10.39	12.91	13.00	13.63		
MnO	0.24	0.28	0.23	0.29	0.31	0.28	0.22	0.30	0.28	0.30	0.27	0.24	0.06	0.05
MgO	13.04	12.01	13.39	10.77	10.96	10.80	11.08	11.31	11.83	10.36	10.87	10.71	< .01	< .01
CaO	11.65	11.29	11.58	11.45	11.48	11.28	11.83	11.00	11.37	11.82	11.89	11.96	28.97	28.72
Na_2O	1.47	1.78	1.68	1.72	1.16	1.62	1.24	1.46	1.69	1.79	1.62	1.58	0.03	0.02
K_2O	0.31	0.51	0.29	0.45	0.32	0.42	0.36	0.44	0.41	0.26	0.39	0.36	0.01	0.01
CoO	<.01	<.01	<.01	<.01	<.01	<.01	<.01	<.01	<.01	<.01	<.01	<.01	<.01	<.01
NiO	0.11	0.13	<.01	0.12	0.31	0.09	<.01	0.02	<.01	<.01	<.01	<.01	<.01	<.01
CuO	0.02	0.02	<.01	0.02	0.02	0.01	<.01	<.01	<.01	<.01	0.02	<.01	0.02	0.03
Total	96.17	96.25	96.45	97.16	98.29	96.10	96.38	94.63	96.31	94.56	95.06	94.67	100.38	100.91
Fe_2O_3 max	4.68	5.43	2.22	4.98	6.14	5.35	1.09	6.46	7.94	3.21	3.15	1.97	Sphene formulae	
Fe_2O_3 min	0.01	0.00	0.00	0.00	0.09	0.00	0.00	0.22	2.37	1.38	1.32	0.76	to 5 oxygens	
Fe^{+3} max	.517	.604	.244	.544	.670	.599	.121	.730	.882	.368	.359	.227	Si .963	.969
Fe^{+3} min	.001	.000	.000	.000	.010	.000	.000	.025	.266	.159	.151	.087	Ti .986	.985
Si	6.785	6.589	6.994	6.595	6.702	6.582	6.924	6.656	6.425	6.411	6.544	6.605	Al .048	.052
Al^{IV}	1.215	1.411	1.006	1.405	1.298	1.418	1.076	1.344	1.575	1.589	1.456	1.395	Cr .001	.001
Σ	8.000	8.000	8.000	8.000	8.000	8.000	8.000	8.000	8.000	8.000	8.000	8.000	Fe .011	.012
Al^{VI}	0.568	0.615	0.580	0.595	0.662	0.624	0.715	0.570	0.495	0.625	0.536	0.562	Mn .002	.001
Ti	0.038	0.054	0.032	0.068	0.060	0.073	0.038	0.055	0.070	0.093	0.089	0.091	Ca 1.014	.998
Fe^{+3}	0.260	0.305	0.122	0.279	0.342	0.302	0.061	0.380	0.576	0.263	0.255	0.157	Na .002	.001
Fe^{+2}	1.235	1.328	1.312	1.631	1.511	1.552	1.707	1.406	1.203	1.620	1.622	1.721	K .000	.000
Mn	0.030	0.035	0.029	0.037	0.038	0.036	0.026	0.038	0.035	0.039	0.035	0.031	Cu .000	.001
Mg	2.869	2.663	2.925	2.390	2.387	2.413	2.451	2.551	2.621	2.360	2.463	2.438	3.03	3.02
Y	5.000	5.000	5.000	5.000	5.000	5.000	5.000	5.000	5.000	5.000	5.000	5.000		
Fe^{+2} M_4	0.075	0.087	0.035	0.080	0.094	0.086	0.018	0.100	0.088	0.030	0.031	0.020		
Ca	1.842	1.800	1.819	1.826	1.798	1.812	1.881	1.784	1.811	1.936	1.936	1.957		
Na^{M_4}	0.083	0.113	0.146	0.094	0.108	0.102	0.101	0.116	0.101	0.034	0.033	0.023		
X	2.000	2.000	2.000	2.000	2.000	2.000	2.000	2.000	2.000	2.000	2.000	2.000		
Na^{A}	0.338	0.400	0.331	0.402	0.221	0.369	0.256	0.312	0.386	0.496	0.444	0.445		
K	0.058	0.097	0.054	0.085	0.060	0.080	0.068	0.085	0.078	0.051	0.076	0.070		
A	0.396	0.497	0.385	0.487	0.281	0.449	0.324	0.397	0.464	0.547	0.520	0.515		
A % (1)	23.4	24.6	25.0	24.5	16.7	22.8	21.6	21.4	21.7	25.2	25.9	26.6		
AL_4 % (1)	71.7	69.8	65.5	70.8	76.9	72.0	71.7	72.4	73.6	73.2	72.5	72.2		
NAM_4 % (1)	4.9	5.6	9.5	4.7	6.4	5.2	6.7	6.2	4.7	1.6	1.6	1.2		

The following conditions apply to the hornblende and sphene analyses:-

20 kv acceleration potential

counting time 80 seconds

crystal spectrometers

standards:-

Si - wollastonite
Ti - pure Ti
Al - orthoclase
Cr - pure Cr
Fe - pure Fe
Mn - pure Mn
Mg - olivine
Ca - wollastonite
Na - orthoclase
K - orthoclase
Co - pure Co
Ni - pure Ni
Cu - pure Cu

Corrections for dead-time, drift, background by programs in Bowles (1975), and for mass-absorption by programs of Mason, Frost and Reed (1969).

(1) End member components used to classify amphiboles following the procedure of Papiche, Cameron and Baldwin (1974).

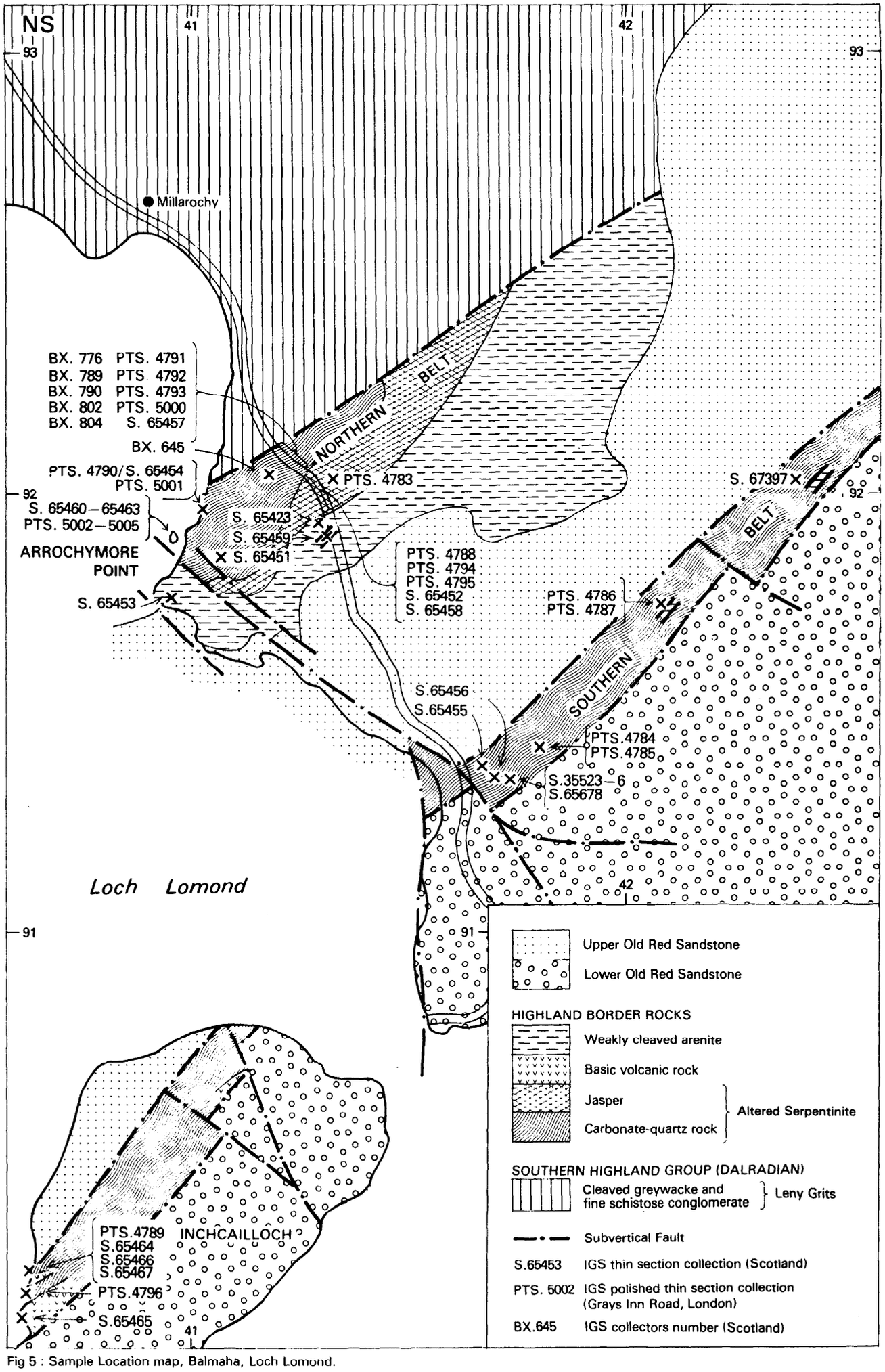

Fig 5 : Sample Location map, Balmaha, Loch Lomond.

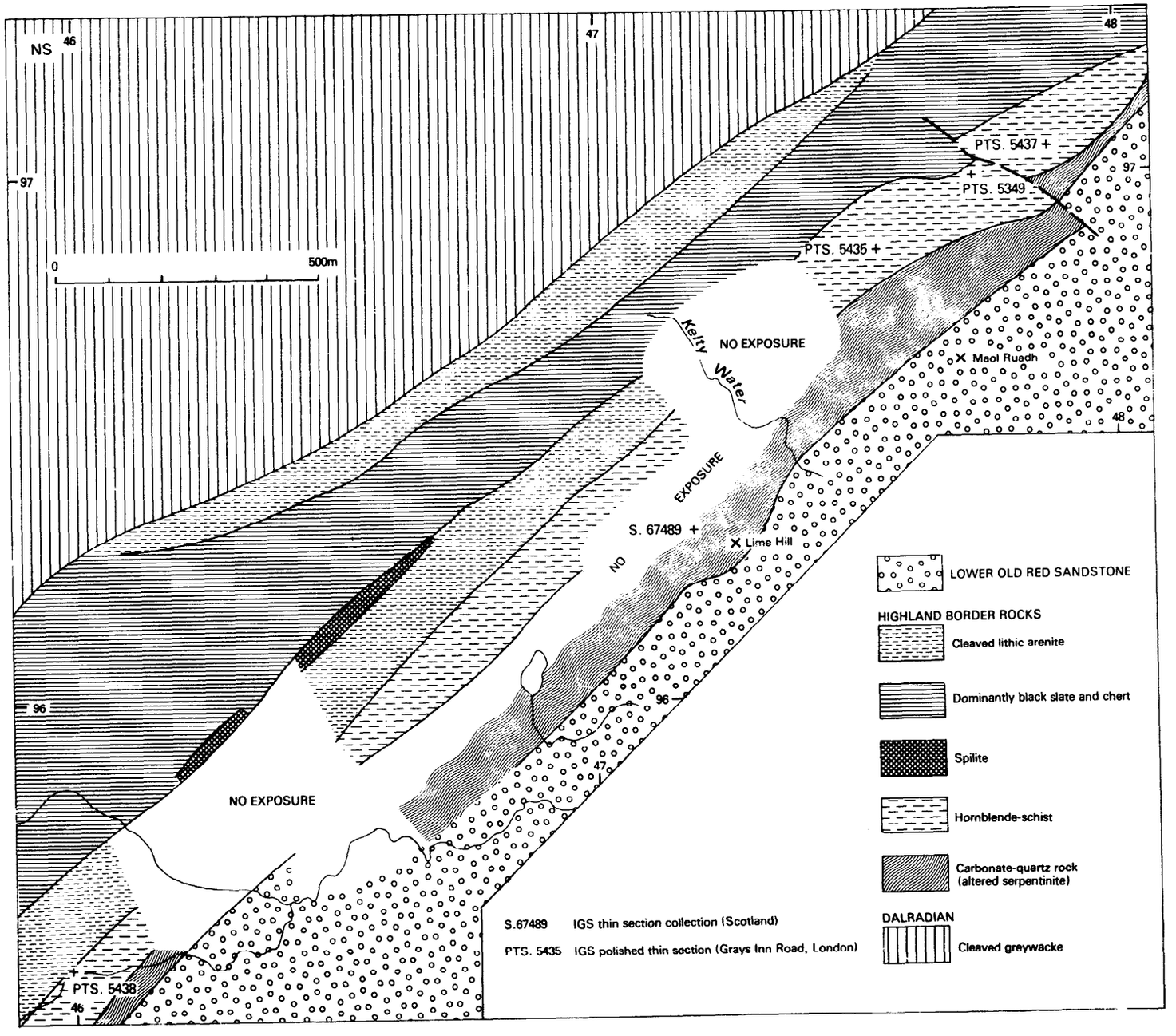

Fig 6: Sample Location map, Aberfoyle Forest.

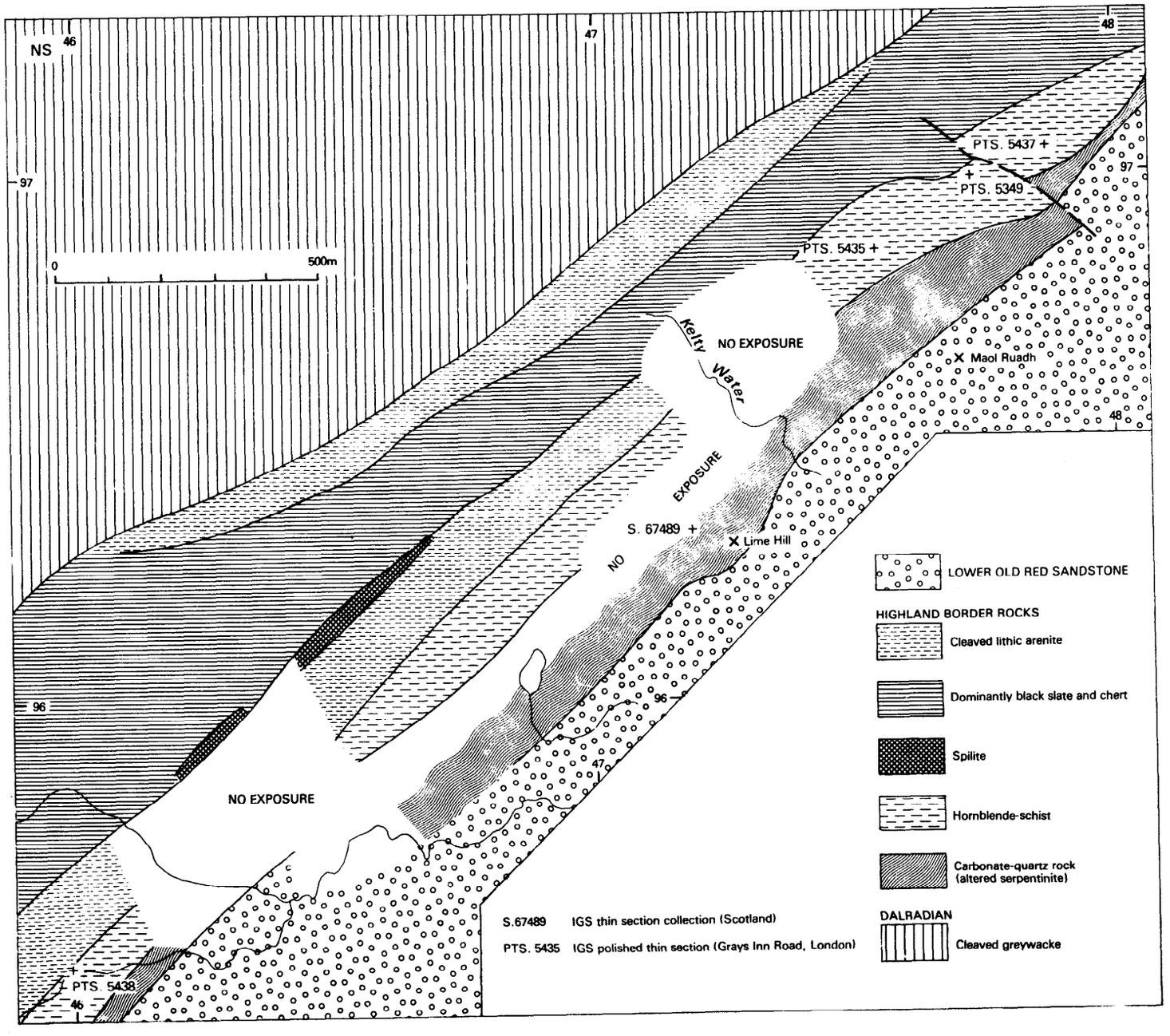

Fig 6: Sample Location map, Aberfoyle Forest.

TABLE 8

Composition of Amphiboles from Creinch, Loch Lomond

(Analyst N J Fortey)

	PTS 5436 (BX1043)							
	1	2	3	4		A		B
SiO_2	55.64	55.08	55.59	55.31		54.73		54.9
TiO_2	0.03	0.01	0.05	0.02		0.21		0.21
Al_2O_3	0.53	0.67	0.66	0.51		1.46		1.2
Cr_2O_3	0.91	0.91	0.74	0.78		-		0.50
FeO*	4.48	4.32	4.35	4.21		9.60		2.8
MnO	0.23	0.19	0.22	0.19		0.16		0.08
MgO	18.05	18.24	16.55	19.68		17.94		25.3
CaO	12.74	12.68	12.62	12.14		12.76		12.7
Na_2O	0.53	0.50	0.47	0.47		1.44		0.6
K_2O	0.07	0.07	0.06	0.06		tr		0.0
CoO	0.01	0.02	0.01	0.01	H_2O+	2.27	H_2O+	0.93
NiO	<0.01	0.02	0.01	0.01			H_2O-	0.27
CuO	0.02	0.01	0.01	0.01			Fe_2O_3	0.5
Total	93.24	92.72	93.33	93.39		100.57		100.0

* Total Fe expressed as FeO

Si	8.134	8.098	8.096	8.048
Al^{iv}	0.000	0.000	0.000	0.000
Z	8.134	8.098	8.096	8.048
Al^{vi}	0.091	0.116	0.113	0.087
Ti	0.003	0.001	0.005	0.002
Fe^{iii}	0.000	0.000	0.000	0.000
Fe^{ii}	0.548	0.531	0.530	0.512
Mn	0.028	0.024	0.027	0.023
Mg	3.934	3.997	4.027	4.268
Y	4.604	4.669	4.703	4.894
Fe^{ii}	0.000	0.000	0.000	0.000
Ca	1.996	1.998	1.970	1.893
Na	0.004	0.002	2.000	0.107
X	2.000	2.000	2.000	2.000
Na	0.146	0.140	0.102	0.025
K	0.013	0.013	0.011	0.011
A	0.159	0.153	0.113	0.036
O	23	23	23	23

(H_2O excluded)

A and B- Deer et al (1963 pp 251-3, nos 7 and 4 resp.)

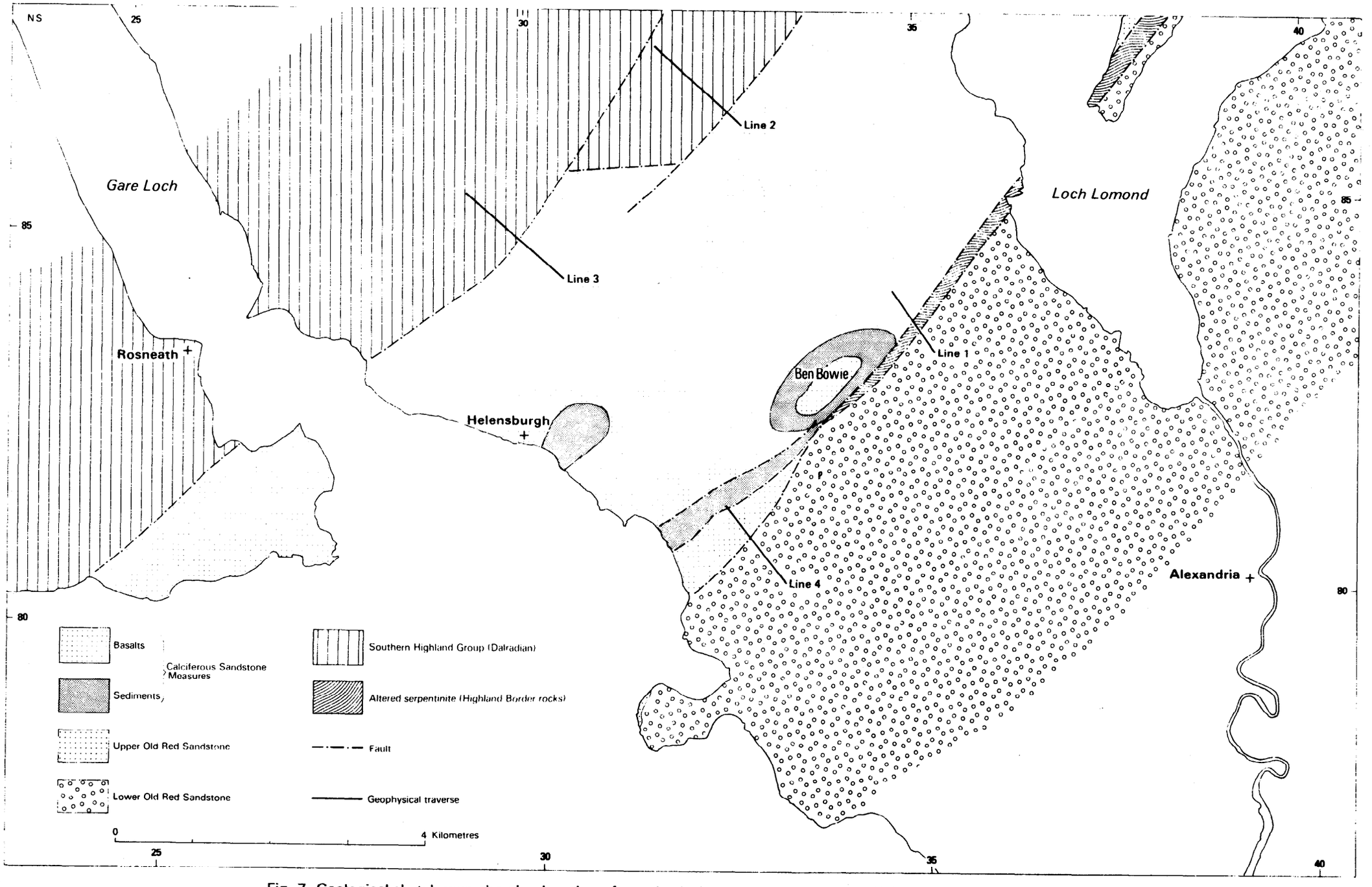

Fig. 7. Geological sketch map showing location of geophysical traverse lines between Helensburgh and Loch Lomond

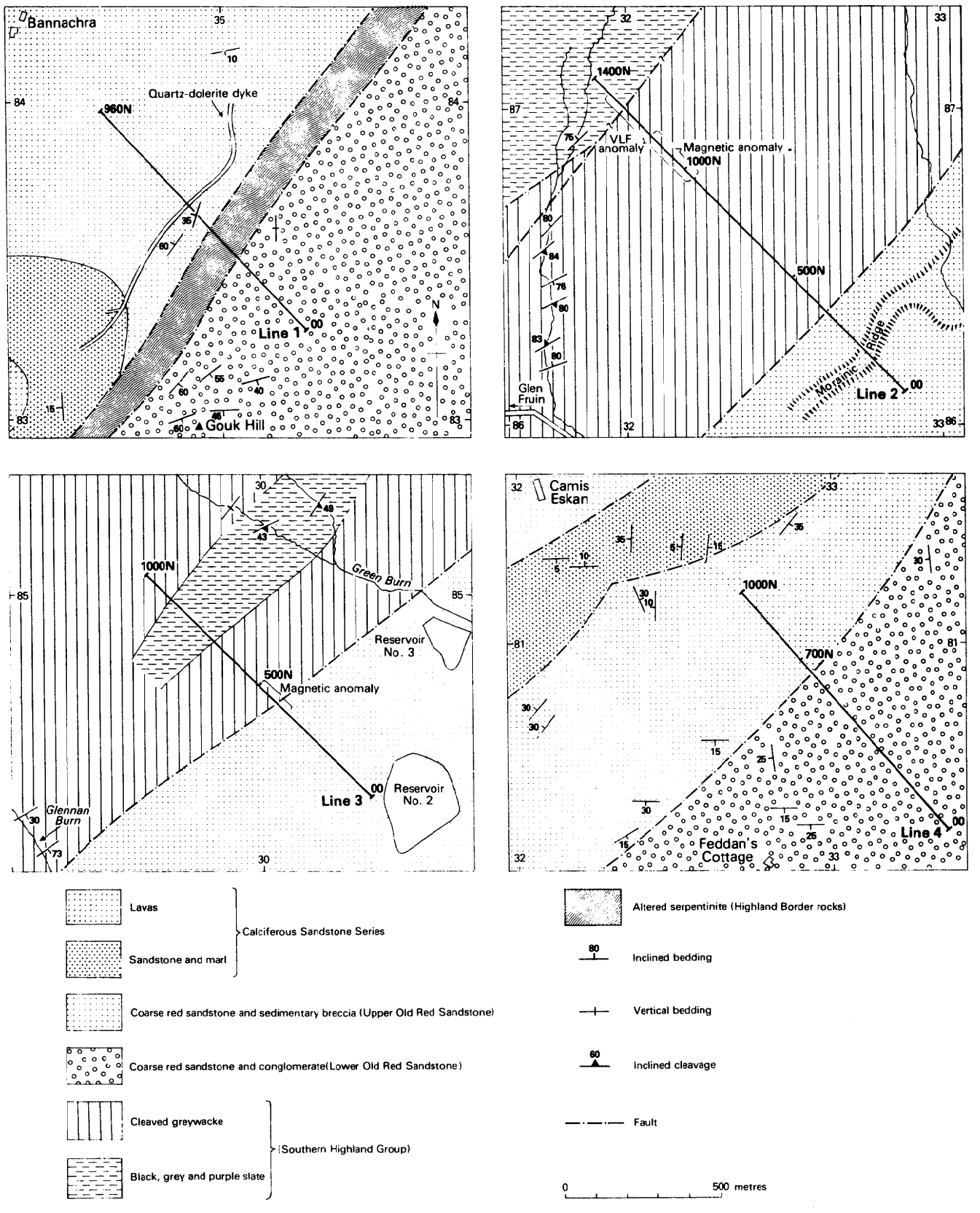

Fig 8. Detailed geology of geophysical traverse lines 1—4.
Geology mainly from I.G.S. 6 inch clean copies (available for reference.)

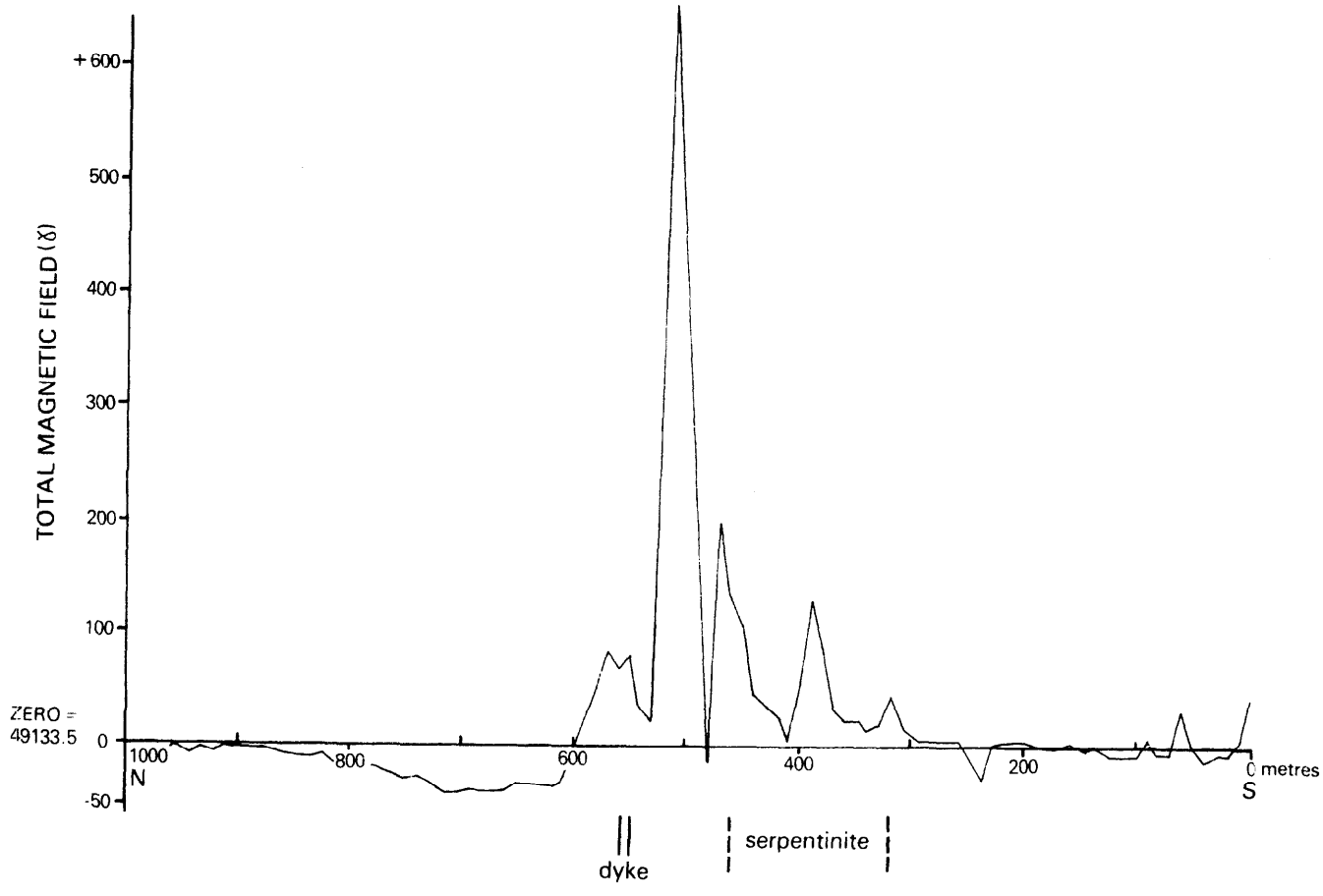

Fig. 9 Geophysical traverse 1. Total magnetic field

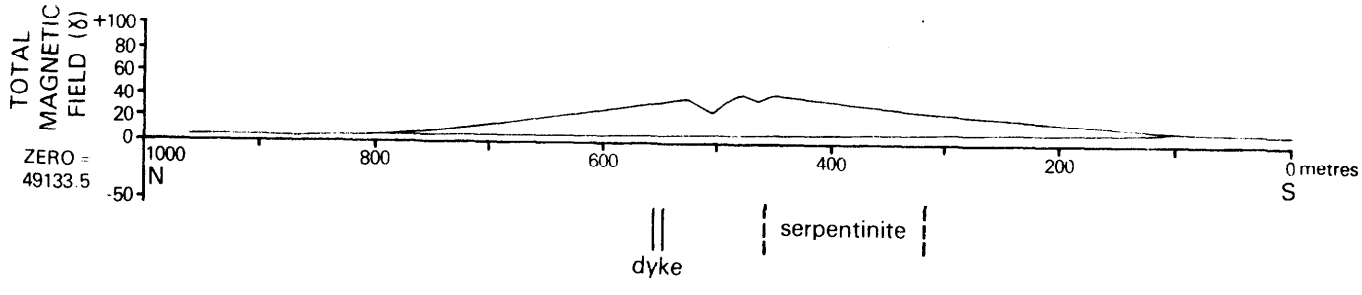

Fig. 10 Geophysical traverse 1. Upward continuation of total magnetic field.
H = 200 metres above ground level

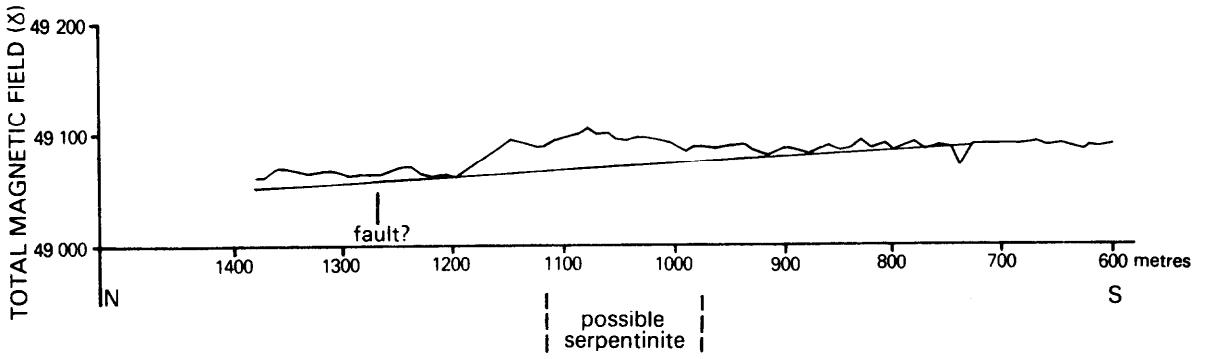

Fig. 11 Geophysical traverse 2. Total magnetic field

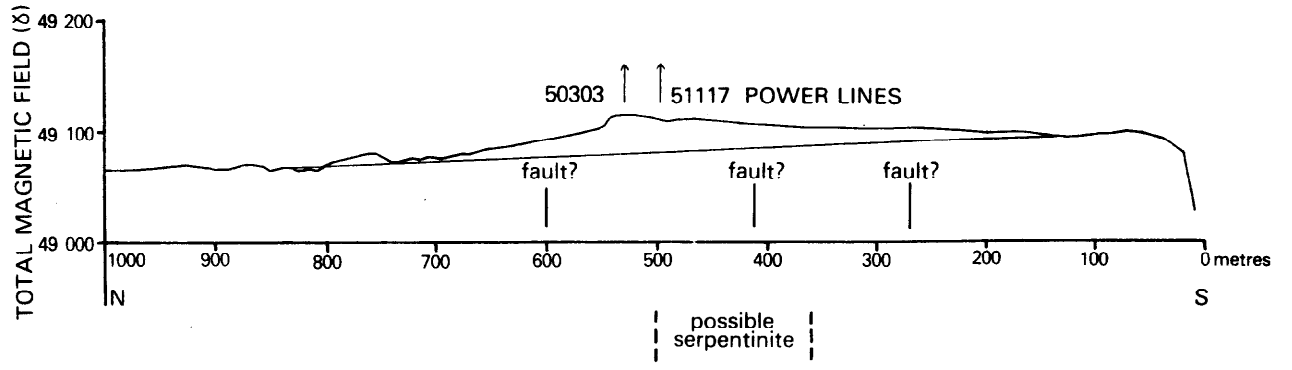

Fig. 12 Geophysical traverse 3. Total magnetic field

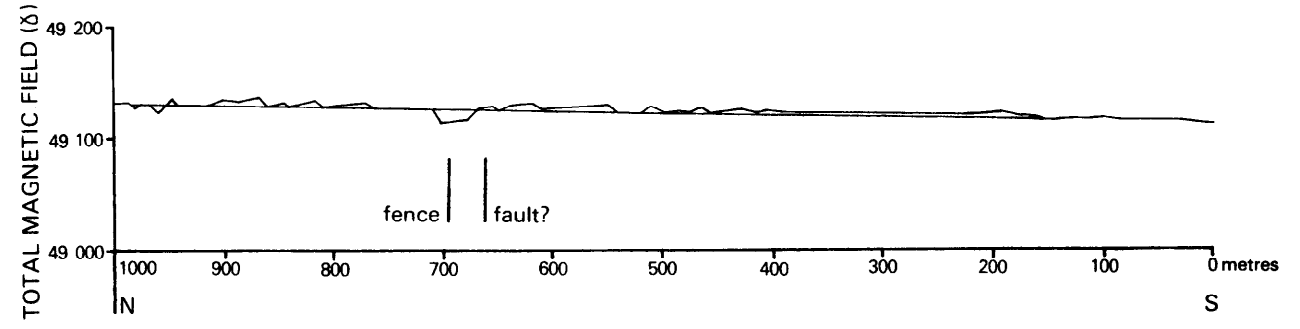

Fig. 13 Geophysical traverse 4 Total magnetic field

The extent to which the Highland Boundary has acted as a channel for metal-bearing solutions is not entirely clear. Baryte veining might have formed by proximity to a metalliferous lineament. Alteration of the serpentinites to carbonate and silica minerals must have required the introduction of large amounts of CO_2 and SiO_2, but the evidence of carbonate-quartz detritus in Highland Border rudites shows that this process began at an early stage in development of the Highland Border rocks. Since these rocks may be allochthonous they were probably altered at a different site to the Highland Border lineament. Therefore, the Highland Boundary may not have had an important role as a channel for mineralised fluids.

ACKNOWLEDGEMENTS

The authors thank their colleagues D. Atkin, L. Ault, B. Beddoe-Stephens, D. J. Bland, B. S. Chaumoo, J. S. Coats, A. R. Date, E. Georgiou, D. J. Morgan and B. R. H. Skilton for providing analytical and mineralogical data. I. H. Hall, North Lowlands Unit, provided helpful advice in the field and M. J. Gallagher kindly commented upon earlier drafts.

REFERENCES

Anderson, E. M. 1942. *The dynamics of faulting and dyke formation, with applications to Britain.* (Edinburgh: Oliver and Boyd.) 191 p.

Anderson, J. G. C. 1947. The Geology of the Highland Border: Stonehaven to Arran. *Trans. R. Soc. Edinburgh*, Vol. 61, pp. 479–515.

Bailey, E. H. and Everhart, D. L. 1964. Geology and Quicksilver deposits of the New Almaden district, Santa Clara County, California. *USGS Prof. Paper* 360.

Barrow, G. 1901. Silurian (?) in Forfarshire and Kincardineshire along the Highland Border. *Q. J. Geol. Soc. London*, Vol. 57, pp. 328–345.

Bowles, J. F. W. 1975. An automatic data-handling system for quatitative X-ray microprobe analysis. *Rep. Inst. Geol. Sci.*, No. 75/9, 14 p.

Campbell, R. 1913. The geology of south-eastern Kincardineshire. *Trans. R. Soc. Edinburgh*, Vol. 48, pp. 923–960.

Deer, W. A., Howie, R. A. and Zussman, J. 1963. *Rock-forming minerals Vol. 2* Chain silicates. (London: Longman.) 379 p.

— — — 1978. *Rock-forming minerals* (2nd edition). Vol. 2A: Single-chain silicates. (London: Longman.) 668 p.

Eckstrand, O. R. 1975. The Dumont serpentinite: a model for control of nickeliferous opaque mineral assemblages by alteration reactions in ultramafic rocks. *Econ. Geol.*, Vol. 70, pp. 183–201.

Groves, D. I., Hudson, D. R. and Hack, T. B. C. 1974. Modification of iron-nickel sulfides during serpentinisation and talc-carbonate alteration at Black Swan, Western Australia. *Econ. Geol.*, Vol. 69, pp. 1265–1281.

Harris, A. L. and Pitcher, W. S. 1975. The Dalradian Supergroup. In **Harris, A. L. and others** (editors). *A correlation of Precambrian rocks in the British Isles. Geol. Soc. London Spec. Rep.*, No. 6, pp. 52–75.

Henderson, W. G. and Fortey, N. J. 1982. Highland Border rocks at Loch Lomond and Aberfoyle. *Scott. J. Geol.*, Vol. 18, pp. 227–245.

Hutchison, C. S. 1974. Laboratory handbook of petrographic techniques. *Wiley-Interscience*, 527 p.

Irvine, T. N. 1967. Chromian spinel as petrogenetic indicator: Part 2, petrologic applications. *Can. J. Earth Sci.*, Vol. 4, pp. 71–103.

Jamieson, R. A. 1980. Formation of metamorphic aureoles beneath ophiolites – evidence from the St Anthony complex, Newfoundland. *Geology*, Vol. 8, pp. 150–154.

Jehu, T. J. and Campbell, R. 1917. The Highland Border rocks of the Aberfoyle district. *Trans. R. Soc. Edinburgh*, Vol. 52, pp. 175–212.

Johnson, C. E. and others. 1980. Geophysical investigation of the chromite-bearing ultrabasic rocks in the Baltasound–Hagdale area, Unst, Shetland Islands. *Mineral Reconnaissance Programme Rep. Inst. Geol. Sci.*, No. 35.

MacGregor, I. D. and Basu, A. 1979. Petrogenesis of the Mount Albert Ultramafic Massif, Quebec. *Bull. Geol. Soc. Am. Part II*, Vol. 90, pp. 1529–1627.

Mason, P. K., Frost, M. T. and Reed, S. J. B. 1969. BM–IC–NPL computer programs for calculating corrections in quantitative X-ray microanalysis. *Nat. Phys. Lab. IMS. Rep. No. 12* (unpublished).

Papicke, J. J., Cameron, K. L. and Baldwin, K. 1974. Amphiboles and pyroxenes: Characterisation of *other* than quadrilateral components and estimates of ferric iron from microprobe data. *Geol. Soc. Am. Abstr. with Progs.*, Vol. 6 (7). October 1974, p. 1053.

Shackleton, R. M. 1957. Downward-facing structures of the Highland Border. *Q. J. Geol. Soc. London*, Vol. 113, pp. 361–392.

Spray, J. G. and Williams, G. D. 1980. The sub-ophiolite metamorphic rocks of the Ballantrae igneous complex, SW Scotland. *J. Geol. Soc. London*, Vol. 137, pp. 359–368.

Wellman, H. W. 1942. Talc-magnesite and quartz-magnesite rock, Cobb-Takaka District, N.Z. *J. Sci. Technol.*, Vol. 24, pp. 103B–127B.

APPENDIX 1

PETROGRAPHY

Brief petrographic notes are given below of rock specimens from the northern and southern belts of Highland Border rocks in the Balmaha/Loch Lomond area. The specimens are grouped under the following headings: Pyroxenite; Serpentinite; Carbonate-Quartz Rocks derived from a) foliated serpentinite, and b) serpentine conglomerate; Jasper; Arenite; Basic Volcanic Rock (Tremolitised).

National Grid References are given with the notes, as are thin section numbers. The latter comprise numbers referring to covered thin sections belonging to the IGS Scottish collection and PTS numbers referring to polished thin sections of the IGS Applied Mineralogy Unit collection. In the main text, carbonate identifications are tablulated in Table 2 and microprobe analyses are given in Tables 3, 6 and 8.

Pyroxenite

PTS 4790 (BX 755A) [NS 4101 9193]

Massive, coarse, granular diopside contains interstitial pockets of serpentine and talc-chlorite associated with which are granules of magnetite. This pale green rock contains veinlets of serpentine which impart a dark green colour to the broken surfaces of the hand specimen. Microprobe analyses (Table 1) indicate chromian diopside, and the rock is believed to represent the pre-serpentinisation ultramafic plutonic stage of genesis.

Serpentinite

S 65461 (BX 821) [NS 4094 9189]

Massive serpentinite containing isolated grains of chromite and small clusters of hematitic granules; also present are sub-parallel hair veinlets of hematitic material cut by later serpentinite veinlets.

S 65462 (BX 822) [NS 4094 9189]

Elongate schistose serpentine fragments set in an elongated framework of carbonate veinlets contain wisps and vein-like patches of probable talc. Hematite patches and isolated chromite grains are accessory constituents.

S 65463 (BX 823) [NS 4094 9189]

Foliated carbonate-serpentinite similar to S 65462 but lacking the talc-like mineral.

PTS 5001 (BX NJ2) [NS 4101 9193]

Foliated, yellow-green serpentinite contains a conformably elongated framework of carbonate veinlets. Hematite and chromite are accessory constituents. Similar to S 65462.

PTS 5003 (BX NJ4) [NS 4094 9189]

Massive, bastitic serpentinite crossed by veinlets of purple-grey hematitic material. Hematite and chromite are accessory constituents in the serpentine itself.

PTS 5004 (BX NJ5) [NS 4094 9189]

Foliated, pale purple serpentinite contains a conformably elongated framework of carbonate veinlets. Talc, hematite and chromite are accessory constituents. Similar to S 65462.

PTS 5005 (BX NJ5A) [NS 4094 9189]

Similar to PTS 5004 but lacking talc. Chromite grains in this rock have incomplete rims of ferritchromite formed before hematite.

Carbonate-Quartz Rocks

(a) derived from foliated serpentinite

S 65451 (BX 646) [NS 4110 9183]

Coarse dolomite rock containing crudely radiate clusters of bladed crystals separated by areas of laminated carbonate oriented perpendicular to the clusters. Opaque microgranules pick out euhedral rhombs in the carbonate. Interstitial patches of microcrystalline quartz and irregular patches of hematite are present.

PTS 4791, PTS 4792 (BX 771) [NS 4122 9207]

Crudely foliated coarse dolomite made up principally of red-stained 'worm-like' dolomite patches consisting either of single strained crystals or of polygranular mosaics. Interstitial patches of microcrystalline quartz are present, together with areas of clear rhombic dolomite. Euhedral blades of hematite are present, and staining by this mineral accounts for the colouration of the rock.

S 65457 A (BX 777A) [NS 4122 9207]

Red-stained coarse dolomite rock showing a folded structure expressed by trails of hematitic granules.

S 65457 B (BX 777B) [NS 4122 9207]

Red-stained dolomite rock made up of areas of coarse, clear carbonate set in stained medium grained matrix. At one side the thin section has a massive texture similar to S 65457A and contains discontinuous strips of hematitic material. Isolated chromite grains are present.

S 65460 (BX 820) [NS 4094 9189]

Fine, mosaic-textured quartz rock in which individual grains are polygonal and show even extinction. Accessory chromite is present.

S 65464 (BX 825) [NS 4061 9014]

Quartz-carbonate rock made up of an irregular patchwork of coarse, ragged carbonate grains and areas of fine quartz mosaic. Straight boundaries, indicating concealed fractures, and quartz and carbonate veinlets are common. Accessory minerals include chromite (partly hematitised) and disseminated hematitic granules.

S 65465 (BX 827) [NS 4062 9010]

Irregularly patchy quartz-dolomite rock containing accessory chromite and hematitic granules. The quartzose component is a fine, intergrown mosaic in which extinction is most uneven and grain boundaries indistinct.

Hexagonal oulined 'bundles' of fibro-radiate quartz form isolated patches. The rock is crossed by a veinlet of fibrous quartz containing patches of unstrained carbonate. Veinlets of unstrained carbonate are also common, and the carbonate component in the rock generally appears to post-date the quartzose.

S 65466 (BX 829) [NS 4064 9021]

Patchy quartz-dolomite rock containing accessory dolomite and hematitic granules. Here a crude foliation is expressed by the patchwork fabric.

S 65467 (BX 830) [NS 4064 9021]

Carbonate-rich patchwork rock with accessory chromite; the quartzose patches have the undulose extinction and indistinct grain boundaries seen in S 65465 and S 65466.

PTS 4789 (BX 831) [NS 4064 9021]

Fine grey quartzose rock containing a relict crenulate laminar fabric largely replaced by coarse dolomite. Minor constituents include chromite, hematitic granules and emerald-green chromian clay/mica material.

PTS 4796 (BX 832) [NS 4064 9021]

Hematite-cherty rock containing accessory chromite, part made over to dolomite containing accessory chromite, partly replaced by fuchsite-like material. The rock is also cut by dolomite veinlets.

S 65468 (BX 833) [NS 3995 8943]

Cryptocrystalline quartz contains isolated quartz 'grains' and dismembered chromite crystals. Carbonatisation has formed coarse dolomitic patches and laminae which may represent an early crenulate fabric.

PTS 5000 (BX NJ1) [NS 4122 9207]
Foliated, hematitic-stained, red dolomite containing cavities, often elongate with the fabric, filled by hematite, calcite and pink baryte. Patches of fine, quartz-rock are also present, and display relict fine banding picked out by opaque micro-granules. Accessory chromite was observed.

Carbonate-Quartz Rocks
(b) derived from serpentine conglomerate
PTS 4784 (BX 650) [NS 4177 9135]
Magnesite-rich rock with minor dolomite shows a relict clastic structure. 'Clasts' of fine quartz-mosaic material are part replaced by the carbonates, and are set in a matrix of similar fine quartz-mosaic also part carbonatised. Many 'clasts' are charged with hematitic granules. Tenuous patches of green (?chromian) clay/mica give a mottled appearance to the hand specimen. Dilational magnesite veins contain central zones of microspherulitic chalcedony.

PTS 4785 (BX 651) [NS 4177 9135]
Pink magnesite mosaic with accessory quartz and dolomite is crossed by magnesite veinlets which include later veinlets with central chalcedony zones. The mosaic contains small isolated relict clasts which in some cases include fine quartz material.

PTS 4786, PTS 4787 (BX 653) [NS 4209 9171]
Fine quartz-rock largely replaced by magnesite displays a complex history. A relict clastic structure is intersected by a ramifying sub-parallel network of dolomite veinlets and later magnesite veins which occur singly and contain central chalcedonic zones. Chromite and hematite are minor constituents.

S 65455 (BX 757) [NS 4169 9136]
Cherty quartz-rock extensively carbonatised but which retains a relict clastic structure and is crossed by carbonate veins.

S 65456 (BX 758) [NS 4178 9134]
Fine carbonate rock with a relict clastic structure and crossed by a network of carbonate veins, one of which has an axial zone of quartz.

PTS 4793 (BX 774) [NS 4169 9135]
Fine quartz-rock part replaced by irregular patches of magnesite. Hematitic staining picks out a relict clastic structure. Accessory chromite is present. Areas of green to purple material on the surfaces of the hand specimen are made up of Cr Ni-bearing mica and clay accompanied hematite.

Jasper
PTS 4783 (BX 647) [NS 4133 9193]
Pure quartz rock save for hematitic granules. A prominent refolded foliated relict structure is present.

S 65452 (BX 648) [NS 4131 9195]
Cherty rock in which a relict texture is preserved by fine to cryptocrystalline patches and disoriented laminated clasts. Veins and patches of chalcedonic material are present, as are accessory chromite grains. The rock is cut by quartz veins containing cavities filled by baryte and hematite.

S 65458 (BX 810) [NS 4131 9195]
Cherty rock in which cryptocrystalline, sometimes laminated clasts are set in a fine to medium-grained matrix. Accessory chromite, chalcedonic patches and quartz veinlets are also present.

PTS 4794 (BX 810A) [NS 4131 9195]
Iron-stained cherty rock crossed by vuggy quartz-veins with pink baryte vug-fills. A relict clastic structure is shown by laminated 'clasts' of medium-grained quartz set in a finer matrix.

PTS 4788 (BX 811) [NS 4131 9195]
Red-stained cherty rock fractured and loosely cemented by hematite, calcite and baryte. The cherty rock has a complex structure in which laminated 'clasts' can be made out. Hematite and chromite are accessory minerals, and veinlets of chalcedonic material are present.

PTS 4795 (BX 812) [NS 4131 9195]
Red-stained cherty rock similar to PTS 4794 and containing accessory chromite.

S 65459 (BX 814) [NS 4131 9195]
Cherty rock with relict crenulate foliated structure. Accessory chromite and hematitic granules are present, and patches of pale chlorite are drawn out with the foliation.

PTS 5002 (BX NJ3) [NS 4094 9189]
Banded cherty rock in which pale bands containing 'schlieren' of chalcedony alternate with red bands rich in grains of hematite. Accessory chromite is present. The rock is cut by quartz veinlets.

Arenite
S 65453 (BX 753) [NS 4095 9177]
Detrital coarse sediment made up of grains of quartz accompanied by grains of opaque material, quartzite, sericitic quartzite, sericitic–chlorite rock and chlorite rock. Several quartz grains display strain-extinction, but there is no evidence of post-depositional deformation.

S 65423 (BX 813) [NS 4131 9195]
Detrital sediment made up of quartz grains accompanied by opaque grains, muscovite and accessory zircon. Although some quartz grains show strain-extinction the rock itself is undeformed. The matrix consists of quartz with sericite and opaque granules. The rock is cut by a quartz veinlet containing a few clay-filled cavities.

Basic Volcanic Rock (Tremolitised)
S 65424 (BX 826) [NS 4061 9014]
Tough green rock with fragmental appearance. The fragments are of pale green chlorite and low-birefringence tremolite which form a felted mass with a crude planar fabric. Turbid carbonate replaces (?ferromagnesian) phenocrysts. The fragments are set in a felsic matrix of small euhedral albite grains, acicular tremolite and carbonate.